January 2012

Spatial and Temporal Variations in the Air-Sea Carbon Dioxide Fluxes of Florida Bay

Christopher Michael Dufore
University of South Florida, chris.dufore@gmail.com

Spatial and Temporal Variations in the Air-Sea Carbon Dioxide Fluxes of Florida Bay

by

Christopher M. DuFore

A thesis submitted in partial fulfillment
of the requirements for the degree of
Master of Science
College of Marine Science
University of South Florida

Major Professor: Robert H. Byrne, Ph.D.
Albert C. Hine, Ph.D.
Kimberly K. Yates, Ph.D.

Date of Approval:
November 30, 2011

Keywords: pH, inorganic carbon, alkalinity, calcium carbonate, salinity

Table of Contents

List of Tables iii

List of Figures v

Abstract vii

Introduction 1
- Global Carbon Cycling 1
- Coastal Carbon Budgets 2
- Carbon Dioxide Flux Measurements 4
- Physical Description of Study Area 4
- Purpose of Study 8

Methods 10
- Measurement of Carbon Dioxide Flux 10
- Collection of Seawater Samples 12
- Total Alkalinity Measurements 13
- Total Dissolved Inorganic Carbon Measurements 15
- CO_2 System Characterization 15

Results and Discussion 17
- Direct Flux Measurements 17
- Spatial Patterns of Fluxes 19
  - Eastern Region 19
  - Central Region 20
  - Northern and Southern Regions 21
- Temporal Patterns of Fluxes 21
  - April 2001 Fluxes 21
  - June 2001 Fluxes 22
  - August 2001 Fluxes 23
  - November 2001 Fluxes 24
  - December 2001 Fluxes 25
  - April 2002 Fluxes 26
  - October 2002 Fluxes 27
  - February 2003 Fluxes 28
  - April 2003 Fluxes 29

Seasonal Patterns of Fluxes 30
Characterization of the Carbonate System: DIC-TA Relationships 32
Relationship Between Measured CO_2 Flux and Calculated ΔpCO_2 35
Predicting ΔpCO_2 37

Conclusions 41

References 43

Bibliography 50

Appendix I: Floating Chamber Specifications 53

Appendix II: Carbon Dioxide System Chemistry 54

Appendix III: CO_2 Flux Data Tables 56

Appendix IV: Carbonate System Data Tables 65

Appendix V: Error in Calculated CO_2 System Parameters 69

List of Tables

Table 1. Average CO_2 fluxes shown in Figure 19. 40

Table A1. CO_2 flux data from 24 stations during the period April 9 to April 12, 2001. 56

Table A2. CO_2 flux data from 24 stations during the period June 12 to June 15, 2001. 57

Table A3. CO_2 flux data from 24 stations during the period August 14 to August 17, 2001. 58

Table A4. CO_2 flux data from 24 stations during the period November 13 to November 16, 2001. 59

Table A5. CO_2 flux data from 24 stations during the period December 11 to December 13, 2001. 60

Table A6. CO_2 flux data from 24 stations during the period April 2 to April 4, 2002. 61

Table A7. CO_2 flux data from 24 stations during the period October 22 to October 24, 2002. 62

Table A8. CO_2 flux data from 24 stations during the period February 11 to February 13, 2003. 63

Table A9. CO_2 flux data from 24 stations during the period April 22 to April 23, 2003. 64

Table A10. Carbonate system parameters from 24 stations during the period April 2 to April 4, 2002. 65

Table A11. Carbonate system parameters from 24 stations during the period October 22 to October 24, 2002. 66

Table A12. Carbonate system parameters from 24 stations during the period February 11 to February 13, 2003. 67

Table A13. Carbonate system parameters from 24 stations during the period April 22 to April 23, 2003. 68

List of Figures

Figure 1.	Map of Florida Bay. General locations of sampling stations.	7
Figure 2.	Map showing sampling locations and regional boundaries.	18
Figure 3.	Average CO_2 flux at each sampling location for all measurements collected during this study.	19
Figure 4.	CO_2 flux during April 2001 field deployment.	22
Figure 5.	CO_2 flux during June 2001 deployment.	23
Figure 6.	CO_2 flux during August 2001 deployment.	24
Figure 7.	CO_2 flux during November 2001 field deployment.	25
Figure 8.	CO_2 flux during December 2001 field deployment.	26
Figure 9.	CO_2 flux during April 2002 field deployment.	27
Figure 10.	CO_2 flux during October 2002 deployment.	28
Figure 11.	CO_2 flux during February 2003 deployment.	29
Figure 12.	CO_2 flux during April 2003 deployment.	30
Figure 13.	Average CO_2 flux at each sampling location for all measurements collected during the wet season (May through October).	31
Figure 14.	Average CO_2 flux at each sampling location for all measurements collected during the dry season (November through April).	32
Figure 15.	Linear relationship between measured total alkalinity and dissolved inorganic carbon collected during the final four sampling trips.	33

Figure 16. Linear relationship between normalized total alkalinity and normalized dissolved inorganic carbon collected during the final four sampling trips. 34

Figure 17. CO_2 flux (mmol m^{-2} day^{-1}) as a function of ΔpCO_2 (µatm). 36

Figure 18. CO_2 flux (mmol m^{-2} day^{-1}) as a function of ΔpCO_2 (µatm). 37

Figure 19. Average CO_2 fluxes obtained using equations 13, 15 and 16 at each sampling location for all F_0 measurements obtained during this study. 39

Abstract

The flux of CO_2 between the ocean and the atmosphere is an important measure in determining local, global, and regional, as well as short term and long term carbon budgets. In this study, air-sea CO_2 fluxes measured using a floating chamber were used to examine the spatial and temporal variability of CO_2 fluxes in Florida Bay. Measurements of dissolved inorganic carbon and total alkalinity obtained concurrently with chamber measurements of CO_2 flux allowed calculation of ΔpCO_2 from flux measurements obtained at zero wind velocity. Floating chamber measurements of ΔpCO_2 were subsequently coupled with wind speed data to provide a simple yet reliable means of predicting absolute flux values. Florida Bay is a marine-dominated, sub-tropical estuary located at the southern tip of the Florida peninsula. Spatial variability within the bay reveals four distinct regions that appear to be affected by a variety of physical, chemical and biological processes. In the eastern part of the bay, the waters tend to be oversaturated with respect to CO_2, likely due to the input of freshwater from Taylor Slough. The central portion of the bay is characterized by a number of extremely shallow semi-isolated basins with limited exchange with the rest of the bay. This area is typically undersaturated with respect to CO_2 and provides a sink for atmospheric CO_2. Both the northern and southern regions were highly variable both spatially and temporally.

Introduction

Global Carbon Cycling

Atmospheric carbon dioxide (CO_2) is an important greenhouse gas that absorbs infrared radiation from the earth. As such, CO_2 plays an important role regulating the earth's climate. A variety of anthropogenic activities, including combustion of fossil fuels, deforestation, and cement production, contribute to CO_2 increases in the atmosphere (Houghton, 2003; Marland et al., 2006; Le Treut 2007). Observations of CO_2 in ice cores (Neftel et al., 1985; Etheridge et al., 1996; MacFarling Meure et al., 2006) and direct measurements of CO_2 concentrations in the atmosphere demonstrate that levels increased from around 280 ppm in 1750 to nearly 380 ppm by 2005 (Keeling and Whorf, 2005; Denman, 2007). By 2100 global temperatures are predicted to increase by as much as 3.1˚C relative to the 1980-1999 global mean due to increasing levels of atmospheric CO_2 (Meehl et al., 2007).

Interactions of the atmosphere and the ocean have major implications in controlling atmospheric CO_2 levels. Model results for the period between 2000 and 2005 indicate that the global ocean acted as a net sink for atmospheric CO_2, sequestering approximately 30% of the CO_2 released into the atmosphere from fossil fuel combustion and cement production (Le Quéré et al., 2003; Denman, 2007). Oceanic uptake of CO_2 is related to its exceptional aqueous solubility and its reaction with seawater. Carbon

dioxide is the most abundant of the minor, or trace, atmospheric gases and, subsequent to dissolution in seawater, reacts to form carbonic acid (H_2CO_3). Carbonic acid then dissociates to form bicarbonate (HCO_3^-) and carbonate (CO_3^{2-}) ions that together constitute more than 95% of the dissolved inorganic carbon in seawater. These reactions, and the extent of speciation, depend on the pH of the system. Due to both the exceptional solubility of carbon dioxide and its exchange equilibria with bicarbonate and carbonate in seawater, the ocean contains approximately 98% of the total dissolved inorganic carbon in the ocean-atmosphere system (Pilson, 1998).

The global ocean is currently a substantial sink for excess atmospheric CO_2. However, due to the very large difference in the relative sizes of the oceanic and atmospheric CO_2 reservoirs, relatively small changes in the behavior of the ocean can have a large impact on the extent to which the oceans serve as a repository for atmospheric CO_2. Variables and processes that influence regional exchanges of CO_2 between the ocean and the atmosphere encompass the domains of physics, chemistry and biology. Seawater temperature and salinity influence CO_2 solubility and equilibrium behavior, and the relative concentrations of dissolved CO_2, bicarbonate and carbonate are directly controlled by the relative magnitudes of total alkalinity (TA) and dissolved inorganic carbon (DIC). Both of these key variables are strongly influenced by mineral dissolution rates and processes that are biologically controlled – carbonate precipitation, photosynthesis and respiration (Morse and Mackenzie, 1990).

Coastal Carbon Budgets

While the oceans are currently a net sink for excess atmospheric CO_2, many coastal areas, including estuaries, salt marshes, mangrove forests, and coral reefs (Borges,

2005), have been shown to contribute CO_2 to the atmosphere, most notably in areas where remineralization of organic carbon exceeds primary production (Smith and Hollibaugh, 1993). Formation of organic matter by photosynthesis and decomposition of organic matter by respiration (oxidation) play an important role in determining the overall fluxes of carbon through coastal ecosystems. Respiration of organic carbon in coastal systems can have an enhanced significance via inputs of excess terrestrially-derived organic carbon.

A number of studies have shown that estuaries are a significant source of CO_2 to the atmosphere. The majority of this prior work has focused on estuaries that receive significant freshwater input from rivers where pCO_2 values can be as high as 9500 µatm (Frankignoulle et al., 1998; Borges, 2005; Borges et al., 2005). Recently, Jiang et al. (2008) have shown significant differences between river-dominated estuaries and marine-dominated estuaries where freshwater input from precipitation and groundwater may be substantial.

Questions surrounding the role of estuaries as sources or sinks of atmospheric carbon dioxide contribute significantly to uncertainties in the development of global carbon budgets. Time series studies and investigations of the mechanisms that control carbon dioxide exchange at the air-water interface are needed to constrain existing flux models. High frequency CO_2 system variations are especially important in coastal ecosystems due to large diurnal trends in respiration, photosynthesis and calcification. A detailed understanding of these processes on diurnal, seasonal and decadal scales is important in determining the overall contribution of coastal ecosystems to global averages.

Carbon Dioxide Flux Measurements

A variety of laboratory and field-based approaches have been used to investigate gas transfer across the air-water interface. Measurements of bomb and natural ^{14}C have been used to estimate long-term global exchange of atmospheric CO_2 with the oceans (Broecker et al., 1985, 1986, 1995; Cember, 1989). Several investigations have employed wind tunnels to examine relationships between wind speed and gas transfer (Broecker et al., 1978; Jahne et al., 1984; Liss and Merlivat, 1986). Similar approaches have been performed in lakes and rivers using deliberate additions of gas tracers (Wanninkhof et al., 1985; Crusius and Wanninkhof, 2003; Ho et al., In Press). Additional means of measuring gas flux in the field include direct measurements of gas fluxes using floating chambers (Frankignoulle, 1988; Marino and Howarth, 1993). Kremer et al. (2003) provide a general overview of enclosure methods and suggestions for measurement optimization. Design and procedural recommendations of Kremer et al. that have been incorporated in the present study include the use of a low profile apparatus with a large water-surface-area to chamber-volume ratio, and deployments in low to moderate wind conditions with limited fetch and wave activity.

Physical Description of Study Area

Florida Bay is a subtropical lagoonal estuary covering approximately 2200 km^2 at the southern tip of the Florida peninsula (Figure 1). A string of Pleistocene coralline limestone islands, known as the Florida Keys, form a nearly continuous barrier to the Atlantic Ocean along the southeast border. To the west, the bay opens to the waters of the Gulf of Mexico and provides the majority of the tidal mixing. The Everglades, a vast

area at the southern end of the Florida mainland encompassing swamps, marshes, prairies and mangrove wetlands, forms the northern boundary of the bay. Inflow of much of the fresh surface water to Florida Bay occurs via sheet flow starting from a modest topographic high, approximately 2.3 m above mean sea level (Schomer and Drew, 1982). This area, known as Taylor Slough, feeds into approximately 20 creek systems that eventually drain into an area of coastal swamps and lagoons in the northeast portion of the bay (McIvor et al., 1994).

Modifications to this ecosystem date back as far as the late nineteenth century when agricultural expansion in the area began and large areas were drained to expose fertile soil. A New York Times article dated June 12, 1892 underscores the notions of the time; "…but this sugar land is not the ordinary Florida soil. It is land that was for centuries the bottom of lakes. The lakes have been partially drained, and the soil thus exposed is rich and black and will produce sugar cane for a hundred years without any fertilizing." Over time, water management programs were created for agricultural utilization, flood control, and water supply to provide for the expanding population and urbanization that was taking place in southern Florida.

The influence of marine processes on Florida Bay's present geomorphology is thought to have begun about 4,500 ka ago in the southwest portion of the bay where the bedrock lies approximately 3 m below present sea level (Enos and Perkins, 1979). This bed of Pleistocene limestone known as the Miami Formation slopes from northeast to southwest and holds varying amounts of Holocene sediment, composed primarily of biogenic carbonate materials from the skeletal remains of mollusks, foraminifera, polychaetes, bivalves, calcareous algae, and corals (Bosence, 1989a; Bosence, 1989b).

The majority of the sediment is contained in a network of anastomosing mudbanks and mangrove islands that divide the bay into a series of shallow "lakes" or basins (Kelbe et al., 2007). The mudbanks restrict circulation and reduce nutrient availability making water composition within the bay highly variable (Powell et al., 1989).

Physical processes that control water exchange within and between basins include density-driven flow, tides, and wind-driven currents (Nuttle et al., 2000). Water temperature in the bay is a function of air temperature and water level. Average daily air temperatures range between approximately 17˚C to 25˚C, and average daily maximum temperatures consistently exceed 27˚C from March to November (Duever et al., 1994; Obeysekera et al., 1999). Bank temperatures exhibit a mean daily range of 4.5°C, but have a maximum range up to 15°C. In contrast, basin temperatures have a range on the order of 1 to 2°C (Holmquist et al., 1989). Monthly average rainfall data from South Florida reveals a highly seasonal pattern with a wet season that extends from around May to October and a dry season that extends from November to April (Duever et al., 1994; Obeysekera et al., 1999; Lee et al., 2006).

Salinity can vary greatly throughout the bay, and is marked by periods of hypersalinity that can last for many months (Fourqurean and Robblee, 1999). Salinity values exceeding those of typical surface seawater are usually confined to the central (interior) portion of the bay where physical isolation creates areas that are highly sensitive to the balance between evaporation and precipitation (Swart and Price, 2002; Kelbe et al., 2007)). In contrast, it has been shown that freshwater plumes from Shark River Slough travel south around Cape Sable and may enter the western region of the bay (Fourquerean et al., 1993). Swart and Price (2002) used $\partial^{18}O$ values to conclude that

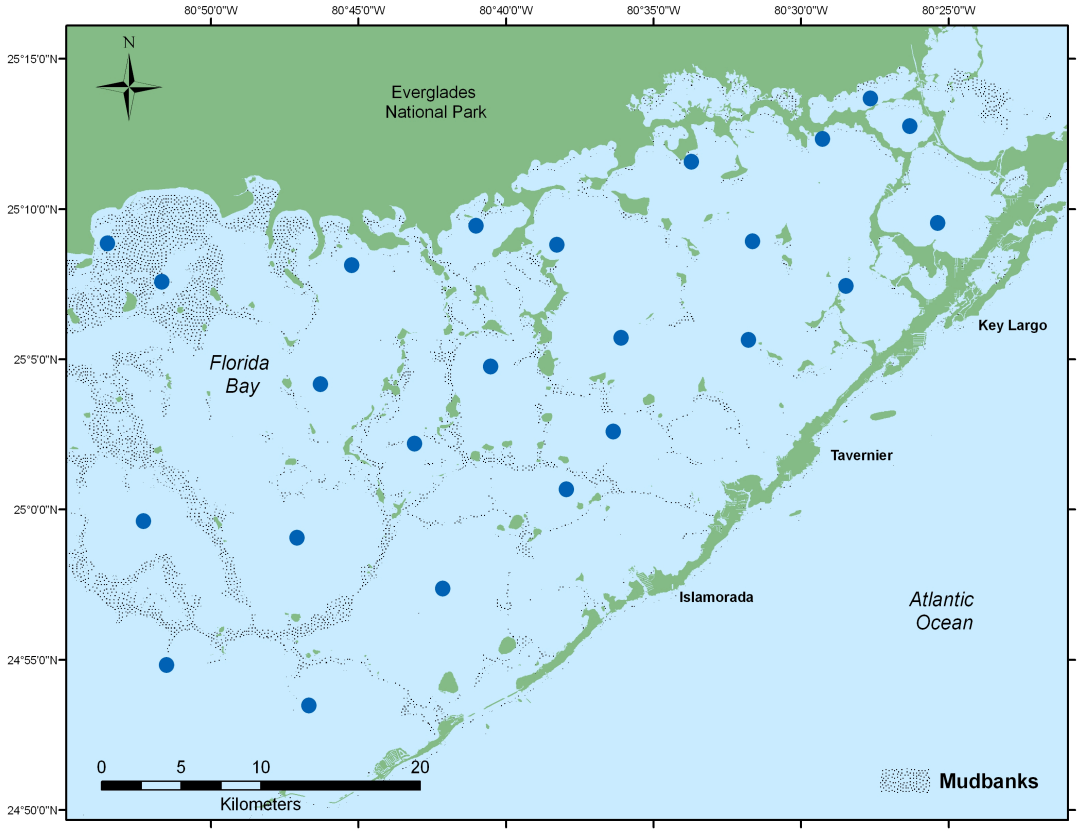

Figure 1. Map of Florida Bay. General locations of sampling stations.

salinity variations in eastern Florida Bay were mainly influenced by input of freshwater from the Everglades and that the dominant influence on salinity in the western part of the bay was precipitation. They further showed that periods of elevated salinity were likely caused by evaporation, especially during the summer months.

The tides of Florida Bay are semi-diurnal with an average range of 60 cm on the Atlantic side of the Florida Keys and at Cape Sable. Inside the first line of mudbanks within the bay, tidal currents are generally less than 15 cm s^{-1} (Wanless and Tagett, 1989). Tidal ranges on the interior of the bay, where water levels and vertical mixing are controlled by wind driven currents, are on the order of 1 cm (Smith, 1997; Fourqurean

and Robblee, 1999). Freshwater flow into the bay is strongly seasonal characterized by a relatively long dry season from November to April, and a wet season from May to October (Schomer and Drew, 1982). More than 80% of annual freshwater input from Taylor Slough and the C-111 canal occurs during the wet season (Hittle, 2001). Using annual rainfall and runoff data collected from 1970 to 1995, Nuttle et al. (2000) concluded that only approximately 10% of freshwater entering Florida Bay is from land runoff and the remainder is from direct rainfall. Swart and Price (2002) further concluded that the proportion of freshwater entering the bay from direct rainfall is >80% in large portions of western Florida Bay and drops steadily to <10% in eastern portions.

The unique habitats of Florida Bay support a variety of flora and fauna. Large populations of wading birds, vast expanses of seagrass, and significant commercial and recreational fisheries are all found in Florida Bay. The bay also serves as a nursery for juvenile fishes and invertebrates (McIvor et al., 1994). Seagrass, dominated by *Thalassia testudinum*, is found throughout the bay, and may also include significant communities of *Halodule wrightii*, and *Syringodium filiforme* (Zieman et al., 1989). Other important components of the benthic community within the bay are the sediment-producing calcareous algae *Halimeda* and *Penicillus*, gorgonians, sponges and corals.

Purpose of Study

Three dominant processes influence carbon fluxes within the waters of Florida Bay: 1) photosynthesis and respiration, 2) carbonate precipitation and dissolution and 3) gas exchange at the air-water interface. The aim of this study was direct measurement of carbon dioxide flux across the air-water interface using a floating flux chamber. Over the

course of nine field trips, between April 2001 and April 2003, flux measurements were made at twenty-four stations in the bay. The goal of the project was to examine the spatial and temporal variability of CO_2 exchange between the atmosphere and the waters of Florida Bay.

Methods

Measurement of Carbon Dioxide Flux

The exchange of CO_2 between the air and the surface waters of Florida Bay was measured using a floating chamber (see Appendix I). The chamber was placed directly on the sea surface, and the partial pressure within this chamber was measured using a LI-COR 6252 infrared gas analyzer. The LI-COR analyzer uses two gas-sampling cells. One cell has an internal CO_2 scrubber, allowing for baseline (zero CO_2 concentration) measurements, and the second cell allows measurements of a standard (span gas) that has a known concentration as well as sample gas for measurement of absolute CO_2 concentrations. Certified gas standards were supplied by Praxair and consisted of air with 500 ppm CO_2.

Prior to each measurement, the bell was positioned into the wind until the signal stabilized (approximately 2 minutes). This allowed determination of the air pCO_2, and purged the system with ambient air. After stabilization of the air pCO_2 signal, the chamber was positioned on the sea surface and the system was sealed with a deflated balloon that was placed over a chamber-vent. Using Tygon tubing and an auxiliary pump attached to the Licor gas analyzer, a closed-loop system was used to circulate air from the floating measurement chamber, through a 1 L flask that contained solid $Mg(ClO_4)_2$, through the gas analyzer cell, and back to the floating chamber. The flask that contained

the magnesium perchlorate was submerged in a cooler filled with ice, and served to remove H_2O from the circulating air. The CO_2 concentration in the chamber was recorded by the Licor analyzer system with a 1 Hz measurement frequency. Each flux measurement required approximately 15 minutes.

CO_2 gas flux, F (mol m^{-2} s^{-1}), across the air-water boundary was calculated using equation 1

$$F = (dpCO_2/dt)(V/RTS) \quad \text{Eq. 1}$$

where ($dpCO_2/dt$) is the change (atm s^{-1}) in pCO_2 with time, V is the gas volume (m^3) within the entire measurement system (chamber, tubes, and analyzer cell), R is the gas constant (atm m^{-3} mol $^{-1}$ K^{-1}), T is the air temperature (K) during the measurement, and S is the sea surface area through which the CO_2 enters or leaves the chamber (Frankignoulle 1988). Through application of the ideal gas law, it is seen that Eq. 1 is equivalent to the following equation (Fick's first law):

$$F = (dn/dt)/S \quad \text{Eq. 2}$$

where n is the number of moles of CO_2 in the measurement system per unit area S (cm^2) per unit of time t (sec).

The flux of CO_2 across an air-water boundary can also be expressed in terms of air-sea differences in CO_2 partial pressures:

$$F = k\ K_o\ (pCO_{2(water)} - pCO_{2(air)}) \quad \text{Eq. 3}$$

(McGillis and Wanninkhof, 2006; Wanninkhof et al., 2009), where k is the gas exchange velocity (m s^{-1}), K_o is the CO_2 solubility coefficient (mol m^{-3} atm^{-1}), $pCO_{2(air)}$ is the partial pressure of carbon dioxide in the gas phase and $pCO_{2(water)}$ is a CO_2 gas phase partial pressure in equilibrium with a seawater sample.

Equation (3) allows interpretation of gas flux measurements calculated via Eq. 1 in terms of air-sea differences in CO_2 partial pressures, and gas transfer velocities (k) for wind velocities (w) equal to zero. As wind velocity is known to exert a dominant influence on environmental air-sea fluxes, the measurements obtained in this work do not provide direct observations relevant to absolute values of gas transfer velocities in the environment. However, considering that the product $k K_o$ will be approximately constant over the small range of temperatures in this study (Wanninkhof, 1992), the measurements obtained in this study can be directly used to provide not only spatial and temporal patterns in air-sea CO_2 fluxes, but also, via equation 3, direct quantitative assessments of $pCO_{2(water)} - pCO_{2(air)}$ Thus, direct flux determinations at zero wind velocity can be viewed as an alternative to determinations of $pCO_{2(water)}$ measurements as one of two or more of the primary CO_2 system variables of seawater.

Collection of Seawater Samples

In addition to measurements of CO_2 fluxes at each of twenty-four study sites between April 2002 and April 2003, water samples were collected in 500 ml borosilicate glass bottles at each station for DIC and TA analysis. Using a peristaltic pump and a 142 mm diameter filtration apparatus, water was pressure-filtered through a 0.45 cellulose nitrate filter until the sample bottle was full. A pipette was used to add 200 µl of a saturated mercuric chloride solution to each bottle to eliminate microbial activity. A small amount of Apiezon® grease was applied to the ground glass stopper and the bottle was sealed. A rubber band and clip were used to ensure a gas-tight fit. Salinity (+/- 0.1) and temperature (+/- 0.1°C) measurements were collected using a WTW LF340 meter

and probe, and three-point salinity calibrations were obtained using USGS standards from the Ocala National Water Quality and Research Laboratory.

Total Alkalinity Measurements

The titration (total) alkalinity (TA) is defined as the number of moles of hydrogen ions equivalent to the excess proton acceptors over proton donors in 1 kilogram of sample (Dickson, 1981). The major components of TA (bicarbonate, carbonate, borate, hydroxide and hydrogen ions) are shown in Eq. 4.

$$TA = [HCO_3^-] + 2[CO_3^{2-}] + [B(OH)_4^-] + [OH^-] - [H^+] \quad \text{Eq. 4}$$

where all concentration terms ([ ]) are the sum of free ions and ion pairs (e.g., $[OH^-]$ includes the OH^- bound to Mg^{2+} and $[H^+]$ includes the H^+ bound to SO_4^{2-} and F^-). It is important to note that this equation does not explicitly show other bases that may contribute to TA, especially, phosphate, silicate and organics. Total alkalinity was determined using the spectrophotometric method of Yao and Byrne (1998). Absorbances were measured with an Ocean Optics USB2000 linear array spectrometer. Titrations were performed in a 6.5 cm^2 open-top glass cell (Hellma Cells, Inc.) placed inside a custom built PVC housing that supported a pair of collimating lenses (Ocean Optics #74-UV). Optical fibers (2 m long and 200 μm in diameter) connected the collimating lenses to the light source and the spectrometer. This system allowed for continuous monitoring of pH whereby titrations could be terminated at relatively high pH (pH ~ 4.5), thereby minimizing additions of excess acid. Sample amount and the mass of added acid were determined gravimetrically using a Denver Instruments PI-214 analytical balance (+/- 0.1

mg). Excess acid concentrations were quantified using the sulfonephthalein indicator bromocresol purple. Solution pH_T ($[H^+]_T$ in moles per kg of solution) was calculated as

$$pH_T = 5.8182 + 0.00129(35\text{-}S) + \log((R(25) - 0.00381/(2.8729 - 0.05104R(25))) \quad \text{Eq. 5}$$

where

$$R(25) = R(t)\{1 + 0.01869(25 - t)\} \quad \text{Eq. 6}$$

and $R(t) = A_{589}/A_{432}$.

Subsequent to purging CO_2 from titrated seawater samples, the alkalinity of the seawater was calculated using the following equation (Yao and Byrne, 1998):

$$A_T M_{SW} = N_A M_A - [H^+]_{ASW} M_{ASW} - [HI]_{total} \Delta(HI) M_{ASW} \quad \text{Eq. 7}$$

where A_T is alkalinity (mol kg^{-1} seawater), M_{SW} is the mass of the seawater sample (kg), N_A is the concentration of the added acid (mol kg^{-1} solution), M_A is the mass of the added acid, $[H^+]_{ASW}$ is the excess hydrogen ion concentration of the acidified seawater (mol kg^{-1} seawater), M_{ASW} is the mass of the acidified seawater calculated as $M_{SW} + M_A$, $[HI]_{total}$ is the total concentration of indicator (mol kg^{-1} acidified seawater), and $\Delta(HI)$ is a term that accounts for the moles of H^+ gained or lost by the indicator in the final acidified seawater relative to the stock indicator solution.

Yao and Byrne (1998) note that the R value of the indicator stock solutions can be adjusted to approximate the R values of the acidified seawater solutions ($R_I \approx 0.3$ at pH $\approx$ 4.8) whereupon the $\Delta(HI)$ term becomes very small (< 0.2 µmol kg^{-1}) and can be ignored. Since pH was continuously monitored using a linear array spectrometer, titrations were terminated near $pH_T = 4.5$, further eliminating the need for calculation of $\Delta(HI)$.

Titrations were conducted using 0.1000 N HCl (+/- 0.0001 N) volumetric standards obtained from Aldrich. At the end of each titration, the solution was purged

with a stream of N_2 gas that had been pre-saturated with H_2O. After purging, final absorbance measurements were obtained, and solution temperatures were measured (+/- 0.01°C) with a Hart Scientific 1521 thermometer.

Total Dissolved Inorganic Carbon Measurements

The total dissolved inorganic carbon (DIC) content of seawater is defined as:

$$DIC = [CO_2^*] + [HCO_3^-] + [CO_3^{2-}]. \quad \text{Eq. 8}$$

DIC was measured using a CM5014 coulometer coupled with a CM5130 acidification module (UIC Inc.). Measurement methodology followed that of DOE (1994). Seawater samples (~20 ml) from newly-opened sample bottles were promptly loaded into a syringe through a small length of tycoon tubing and a 3-way stopcock. Once the sample was loaded in the syringe, the syringe and contents were weighed and the sample was injected through a septum on top of the stripping chamber. The emptied syringe was weighed again and the mass of seawater delivered to the stripping chamber was calculated by difference. The sample was then acidified with 2N $HClO_4$ (~ 5 ml). CO_2 released from the solution was carried to the coulometer with a stream of N_2 gas. The coulometer automatically monitored the progress of the titration until the transmittance of the indicating solution returned to its original value (~15 min.). DIC calculations performed using the coulometer software were initially reported as ppm per sample.

CO_2 System Characterization

All additional carbonate system parameters including pH_T, pCO_2, and the saturation states of aragonite and calcite, were calculated using the TA, TCO_2, salinity

and temperature of collected samples (see Appendix II). It is useful to note that TA and TCO_2 do not vary with temperature and pressure. Calculations were made using the program CO2Sys (version 1.02) developed by Lewis and Wallace (1998), employing carbonic acid dissociation constants, K_1 and K_2, from Mehrbach et al. (1973) as refit by Dickson and Millero (1987), and the bisulphate dissociation constants, K_{SO4}, of Dickson (1990).

Results and discussion

Direct Flux Measurements

The variety of conceptual schemes used to divide Florida Bay into discrete zones have included (a) water quality criteria (Boyer et al., 1997; Nuttle et al., 2000), (b) benthic community structure (Turney and Perkins, 1972; Zieman et al., 1989), (c) bank morphology and dynamics (Wanless and Tagett, 1989) and (d) combined criteria, such as the arrangement of mudbanks, islands and patterns of water movement (Costello et al., 1986). In this study, the Bay is divided into four discrete zones that highlight regional differences in CO_2 flux throughout the bay (Figure 2).

Examination of the average flux collected at each sampling location during this study (Figure 3) shows the strong tendency toward out-gassing across the entire eastern region, but as water moves across the bay from east to west, the trend toward oversaturation diminishes greatly. In the central region, this tendency shifts to undersaturtion of CO_2. The northern and southern regions show a higher degree of variability including the lowest overall flux averages over the study period.

Estuarine systems are generally considered to be net heterotrophic ecosystems, where total respiration exceeds gross primary production, resulting in a net release of CO_2 to the atmosphere (Cai and Wang, 1998; Frankignoulle et al., 1998; Mukhopadhyay et al., 2002; Borges, 2005). A number of studies have focused directly on CO_2 fluxes

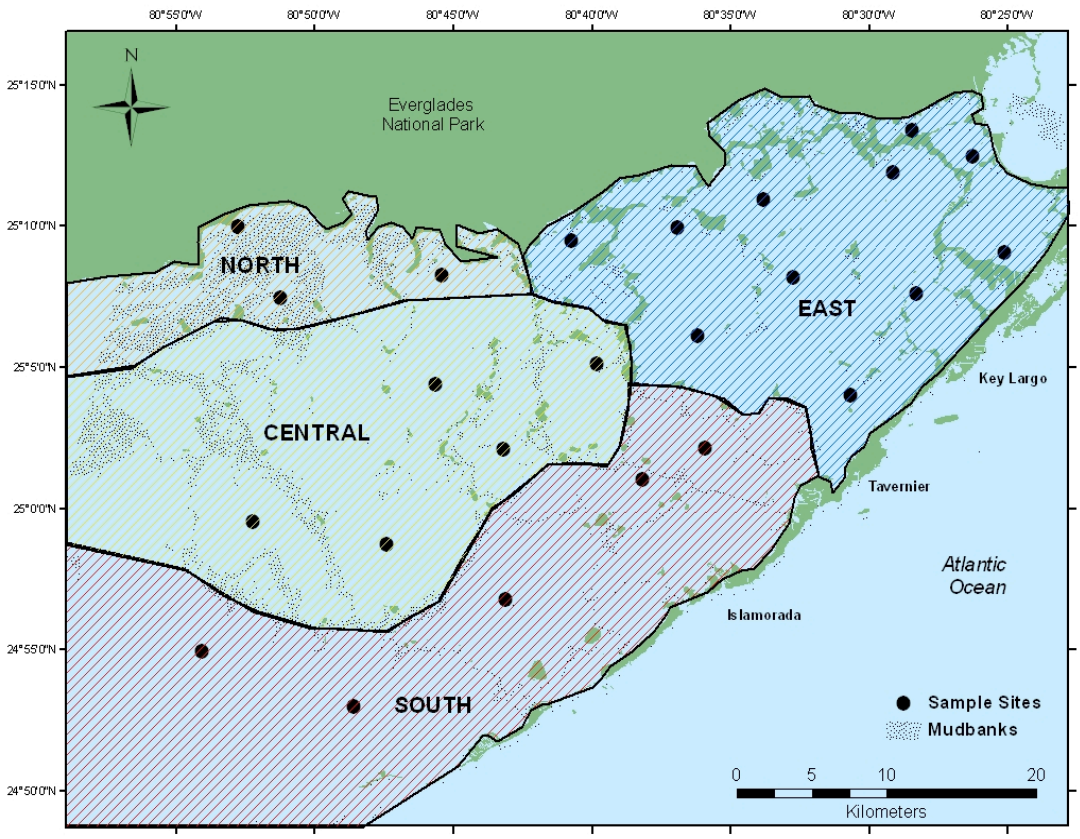

Figure 2. Map showing sampling locations and regional boundaries.

in estuarine systems. Cai and Wang (1998) estimated an average CO_2 flux of 41 mmol m^{-2} d^{-1} at an average salinity of 25, and 164 mmol m^{-2} d^{-1} at an average salinity of 15 in the Satilla River Estuary. Mukhopadhyay et al. (2002) reported a range of 84.4 mmol m^{-2} d^{-1} to -2.78 mmol m^{-2} d^{-1} in the Hooghly estuary. Frankignoulle et al. (1998) measured fluxes in seven European "outer" estuaries with a salinity range of 9-34, and found pCO_2 values that ranged between 240-1330 µatm and mean flux of CO_2 between zero and 50 mmol m^{-2} d^{-1}. In Florida Bay, CO_2 fluxes ranged from 59.9 to -40.3 mmol CO_2 m^{-2} d^{-1} over the entire study period. During the final four sampling trips salinity values

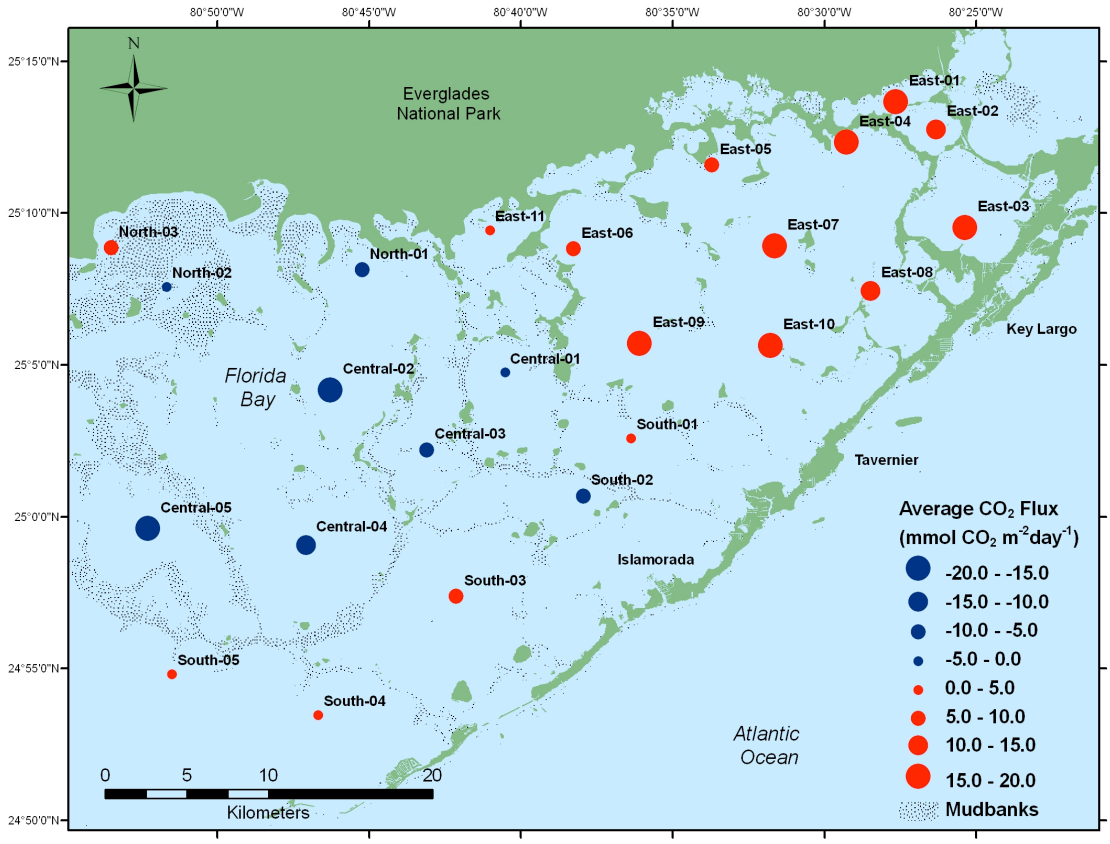

Figure 3. Average CO_2 flux at each sampling location for all measurements collected during this study.

averaged 29.6 and pCO_2 ranged between 65.6 and 798.5 µatm. Figures 4 through 12 show measured fluxes for each of nine sampling trips between April 2001 and April 2003. The results are presented in tabular form in Appendix III.

Spatial Patterns of Fluxes

Eastern Region

In the eastern portion of the bay, a strong tendency for oversaturation of dissolved carbon dioxide in surface waters resulted in a regional average efflux of 13.1 mmol CO_2

m^{-2} d^{-1} over the entire study period. Out of 88 measurements, only four showed an influx of carbon dioxide. This may be attributed to freshwater runoff from Taylor Slough. Indeed, the lowest measured salinity values are found in the eastern portion of the bay. Millero et al. (2001) measured seasonal variation in the carbonate system in Florida Bay and concluded that bacterial and photochemical oxidation of organic matter in the mangrove fringe lowers pH and increases pCO_2 of the water coming into the bay through Taylor Slough. Additionally, large areas of the region are characterized as hardbottom (see Prager and Halley, 1997) containing only sparse benthic communities with relatively low primary production. Physical processes are likely the predominant influence on the chemistry of Bay waters in these areas.

Central Region

In contrast to the strong tendency for CO_2 efflux in the eastern region, the central region showed an overall trend of carbon dioxide undersaturation. Of the 44 samples collected, only six samples show carbon dioxide efflux. The regional average flux for stations observed during the study period was -12.2 mmol CO_2 m^{-2} d^{-1}. Biological processes are likely to exert a strong influence on CO_2 fluxes in this part of Florida Bay. Numerous mudbanks and mangrove islands restrict circulation. The long seawater residence times (multiple months) in this area are favorable to an enhanced influence of biological processes on CO_2 fluxes (Lee et al., 2006). The substantial seagrass cover in this area provides significant primary production that can intensify CO_2 uptake rates (Powell et al., 1989). Similarly, phytoplankton blooms composed mostly of the picoplanktonic cyanobacterium *Synechococcus* have been shown to be common in the central region of the bay when compared to the eastern region (Phlips et al., 1999).

Northern and Southern Regions

Carbon dioxide flux measurements in both the northern and southern regions were highly variable compared to the eastern and central regions. Stations in both areas showed no distinct pattern during individual sampling trips or over the course of the study. Northern sites are characterized as having large areas of open mud flats and extremely shallow water depths. The northern region has also been shown to experience longer and more intense phytoplankton blooms, analogous to those found in the central region. Sampling sites in the south region are strongly influenced by the Atlantic Ocean via tidal exchange through the many passes between the islands of the Florida Keys increasing the likelihood of equilibration with those waters.

Temporal Patterns of Fluxes

April 2001 Fluxes

In April 2001 (Fig. 4), flux measurements at nine of the ten stations measured in the eastern portion of Florida Bay showed considerable efflux, with an average of 18.1 mmol CO_2 m^{-2} d^{-1}. In contrast, other areas of the bay showed a CO_2 influx, with an average of -35.7 mmol CO_2 m^{-2} d^{-1} in the central region, -20.1 mmol CO_2 m^{-2} d^{-1} in the north region, and a modest -2.6 mmol CO_2 m^{-2} d^{-1} in

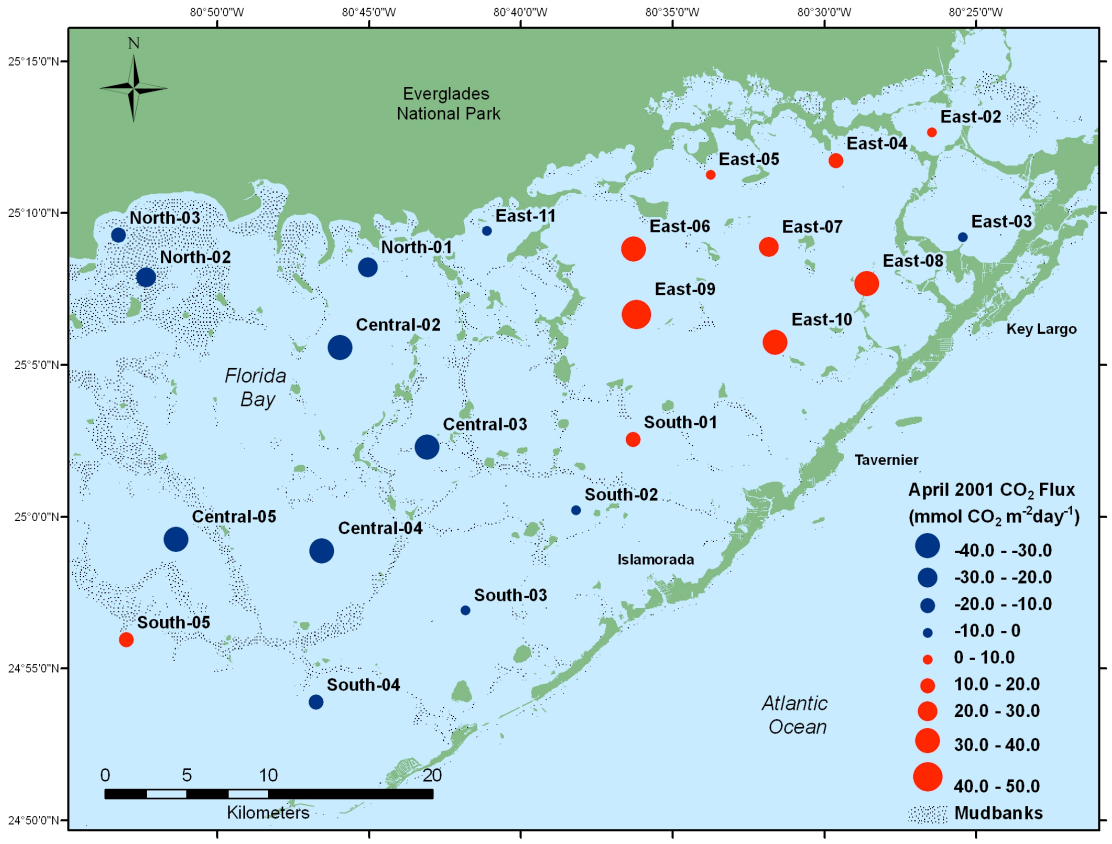

Figure 4. CO_2 flux during April 2001 field deployment.

June 2001 Fluxes

Fluxes during June 2001 (Fig. 5) were relatively low. The east region had an average efflux of 2.8 mmol CO_2 m^{-2} d^{-1} while the north region stations also showed an average efflux with a value of 11.2 mmol CO_2 m^{-2} d^{-1}. Both the central and south region exhibited moderate average influx of -10.3 and -4.9 mmol CO_2 m^{-2} d^{-1} respectively.

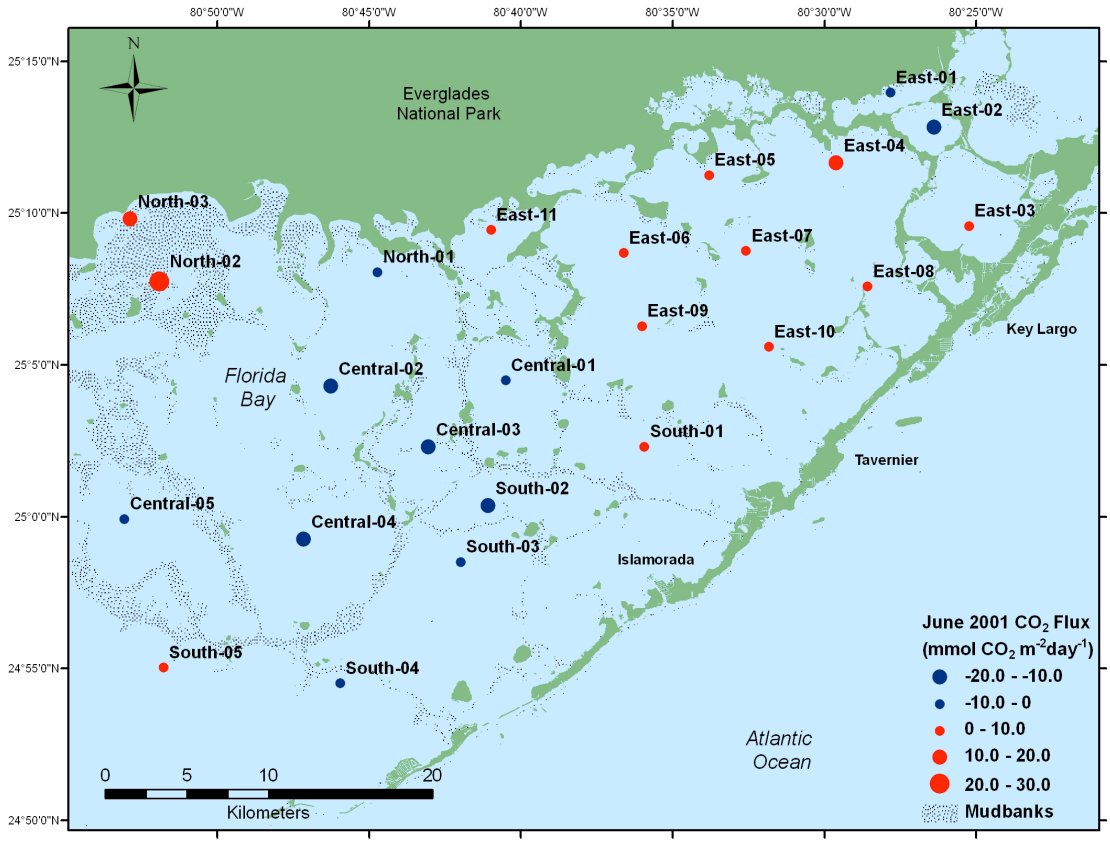

Figure 5. CO_2 flux during June 2001 deployment.

August 2001 Fluxes

The August 2001 data (Fig. 6) showed that all stations in the eastern region had an average efflux of 12.3 mmol CO_2 m^{-2} d^{-1}. Across the entire central region, CO_2 flux showed an average influx of -7.7 mmol CO_2 m^{-2} d^{-1}. The north region was variable, yet stations two and three exhibited the highest uptake rate of the period, with an overall average of -11.8 mmol CO_2 m^{-2} d^{-1}. The southernmost region was variable with an average efflux of 6.8 mmol CO_2 m^{-2} d^{-1}.

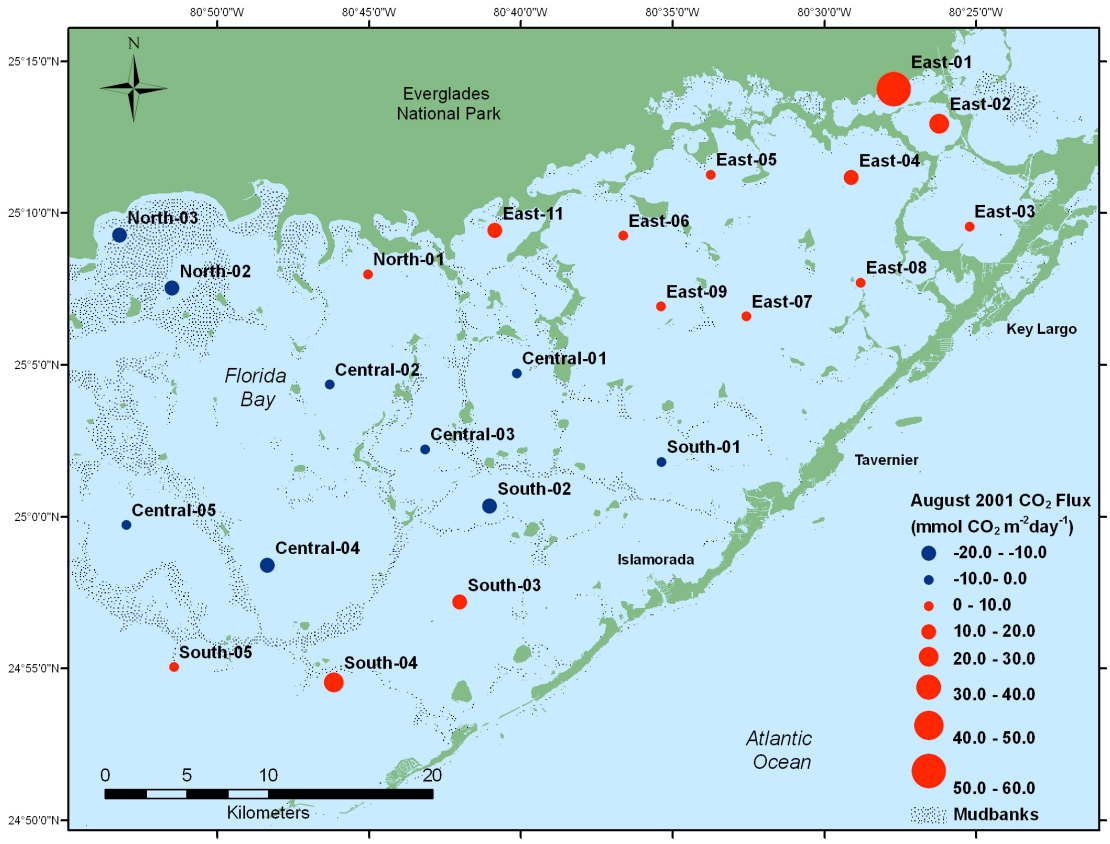

Figure 6. CO_2 flux during August 2001 deployment.

November 2001 Fluxes

November 2001 fluxes (Fig. 7) were again positive throughout the entire eastern region, and ranged between 0.8 and 31.8 mmol CO_2 m^{-2} d^{-1}. The central region had an anomalous efflux of 5.0 mmol CO_2 m^{-2} d^{-1} at station 1 but showed a considerable influx at station 2 of -40.3 mmol CO_2 m^{-2} d^{-1} and a regional average of -15.5 mmol CO_2 m^{-2} d^{-1}. The northern region showed a slight influx of -2.0 mmol CO_2 m^{-2} d^{-1} and the southern region had an overall average efflux of 5.5 mmol CO_2 m^{-2} d^{-1}.

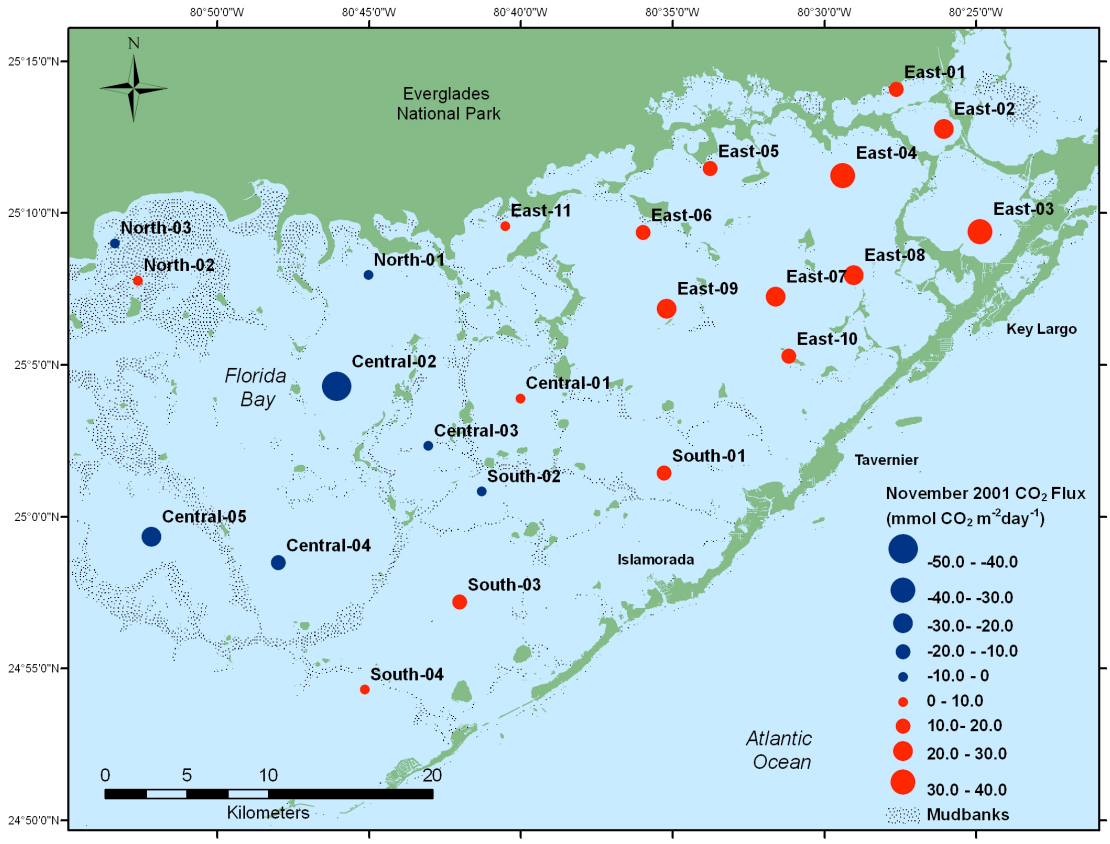

Figure 7. CO_2 flux during November 2001 field deployment.

December 2001 Fluxes

December 2001 fluxes (Fig. 8) were again strongly positive throughout the eastern region of the bay. The average over the entire eastern region was an efflux of 24.1 mmol CO_2 m^{-2} d^{-1}, with an average of 47.3 mmol CO_2 m^{-2} d^{-1} at the three easternmost sites. The average for the central region was -8.6 mmol CO_2 m^{-2} d^{-1}, with one station (Central-04) generating an efflux of 14.9 mmol CO_2 m^{-2} d^{-1}. The southern region had an average efflux of 11.4 mmol CO_2 m^{-2} d^{-1}. The north region was again variable, including the highest efflux measured during the study of 59.9 mmol CO_2 m^{-2} d^{-1} in the Snake Bight Channel (North-03).

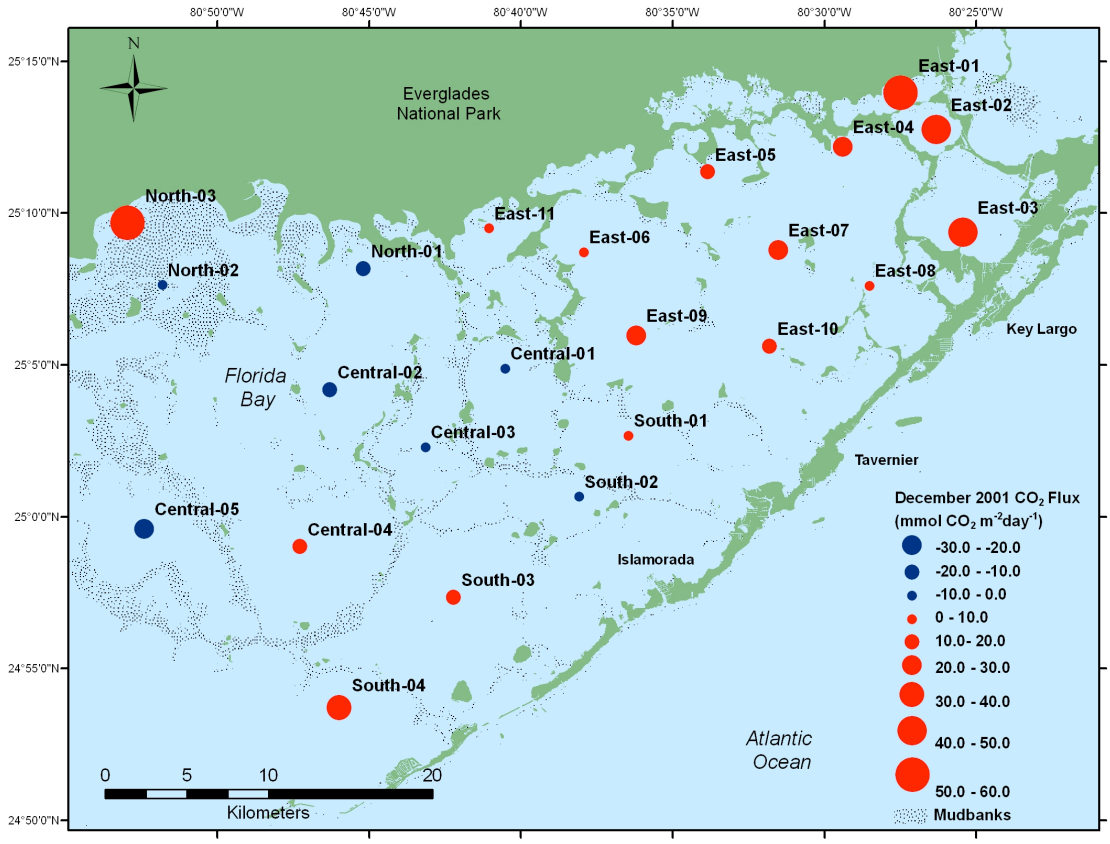

Figure 8. CO_2 flux during December 2001 field deployment.

April 2002 Fluxes

CO_2 flux measurements collected during the April 2002 (Fig. 9) sampling trip were lowest during the entire sampling period. All ten of the eastern region stations exhibited an average CO_2 efflux value over the entire region of 7.4 mmol CO_2 m^{-2} d^{-1}. The north region also showed a modest efflux, averaging 2.3 mmol CO_2 m^{-2} d^{-1}. The central region had an average influx of -3.9 mmol CO_2 m^{-2} d^{-1}, while the south region averaged near neutral at 0.3 mmol CO_2 m^{-2} d^{-1}.

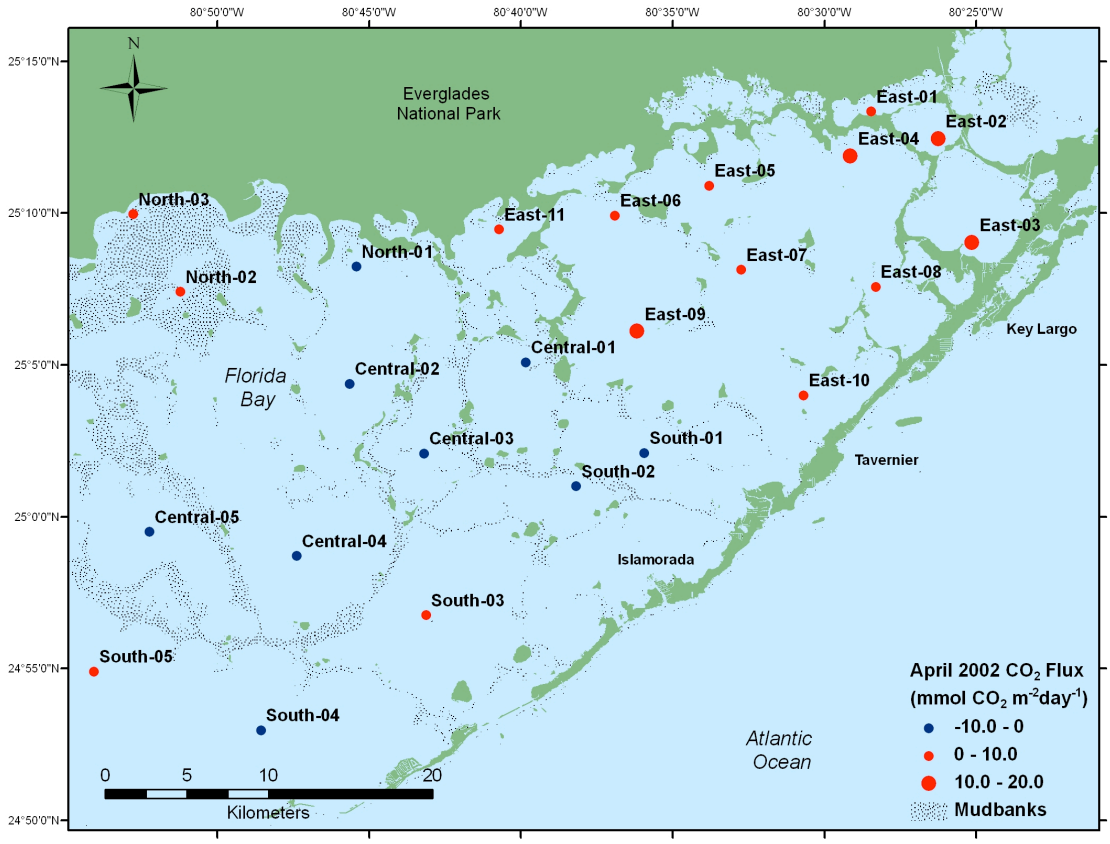

Figure 9. CO_2 flux during April 2002 field deployment.

October 2002 Fluxes

CO_2 flux measurements collected during October 2002 (Fig. 10) continued to show the east region as a source of CO_2 with a regional average of 8.6 mmol CO_2 m^{-2} d^{-1}. In the central region, a relatively high positive flux (Central-04) caused the only positive average efflux in the central region of 0.5 mmol CO_2 m^{-2} d^{-1}. All three stations in the north had an average influx of -4.8 mmol CO_2 m^{-2} d^{-1}. All stations in the southern region had an overall average efflux of 7.9 mmol CO_2 m^{-2} d^{-1}.

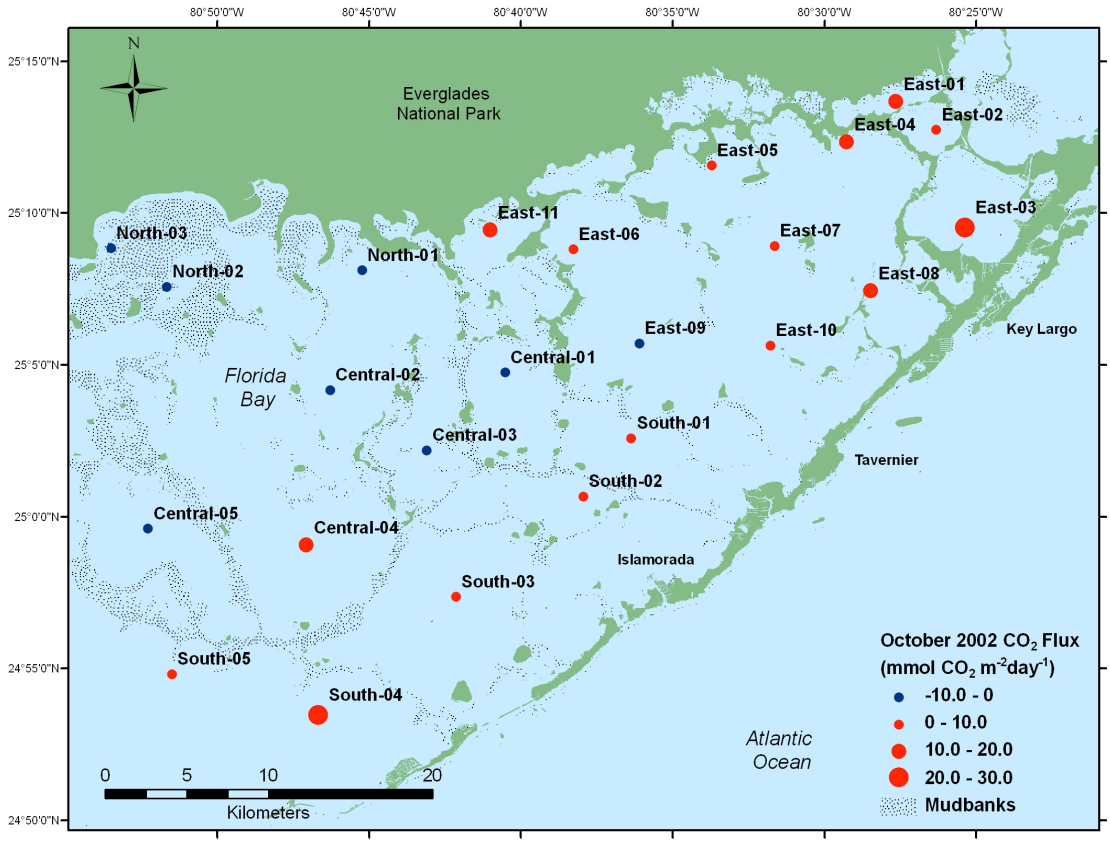

Figure 10. CO_2 flux during October 2002 deployment.

February 2003 Fluxes

February 2003 (Fig. 11) was the coldest period during the entire study. Air temperatures averaged 19.6 ˚C with the bay as a whole releasing CO_2 to the atmosphere. The eastern region averaged 14.3 mmol CO_2 m^{-2} d^{-1}, the north 13.2 mmol CO_2 m^{-2} d^{-1}, and the south 7.8 mmol CO_2 m^{-2} d^{-1}. Only the station in Rabbit Key Basin (Central-05), with a measured influx of -10.6 mmol CO_2 m^{-2} d^{-1}, showed uptake of CO_2.

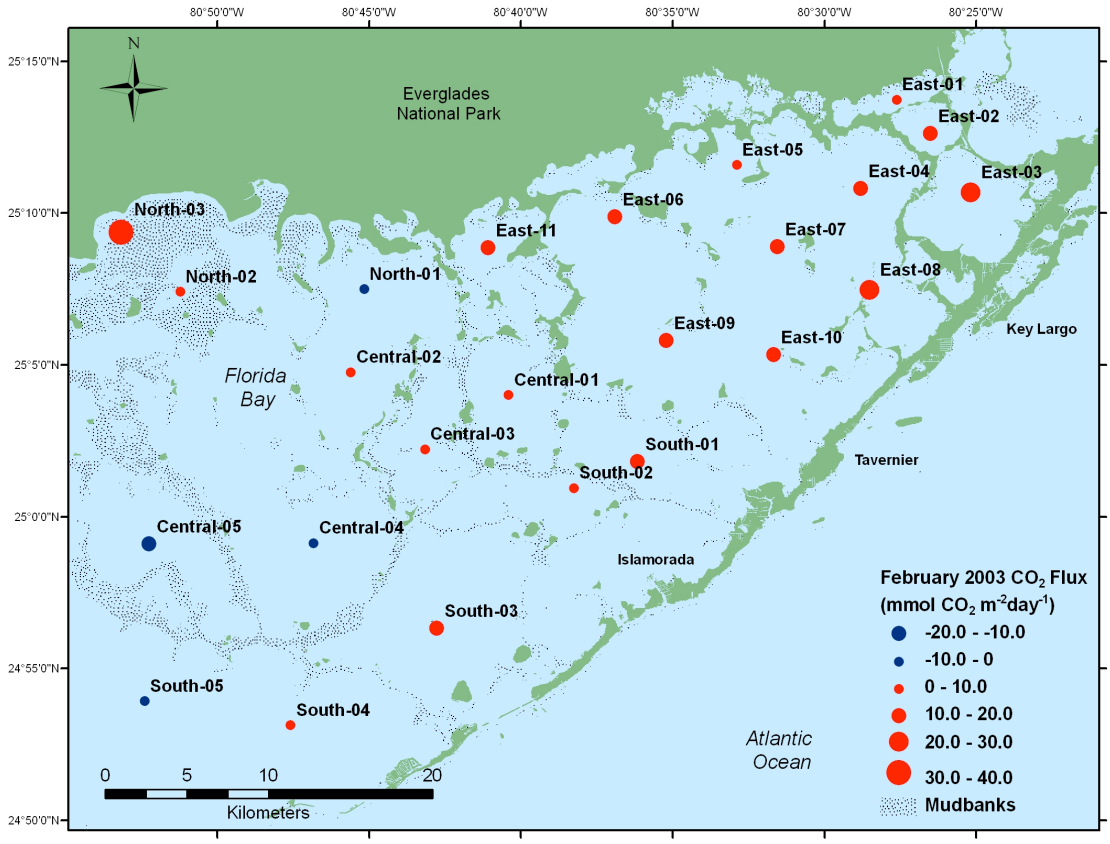

Figure 11. CO_2 flux during February 2003 deployment.

April 2003 Fluxes

During the final field trip, conducted in April 2003 (Fig. 12), a strong tendency for CO_2 efflux was again seen in the eastern region of the bay. The eastern region flux average was 10.3 mmol CO_2 m^{-2} d^{-1}. Stations in the central and southern regions averaged -27.7 and -17.8 mmol CO_2 m^{-2} d^{-1} respectively. The north regions average was 6.0 mmol CO_2 m^{-2} d^{-1}.

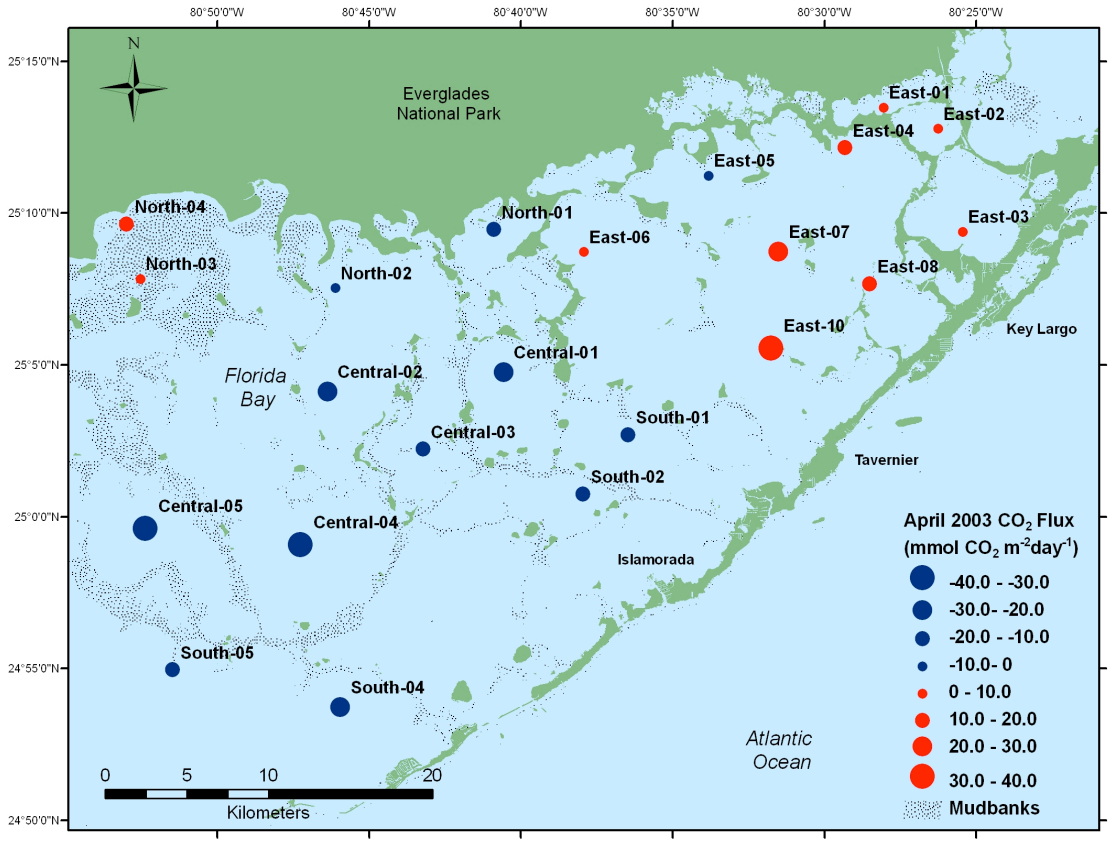

Figure 12. Measured CO_2 flux collected during April 2003 field deployment.

Seasonal Patterns of Fluxes

Seasonal differences in CO_2 flux measurements suggest that biological and physiochemical processes may have an effect on the carbon dioxide system in Florida Bay. During the wet summer months (Fig. 13), average flux measurements show a similar pattern to those collected during the dry winter months (Fig. 14), however, the increased magnitude of the fluxes in the dry season suggests that the enhanced importance of processes such as calcification and photosynthesis may impact bay water chemistry. In addition, longer residence times, especially in the central and east regions, during the dry season may play an important role.

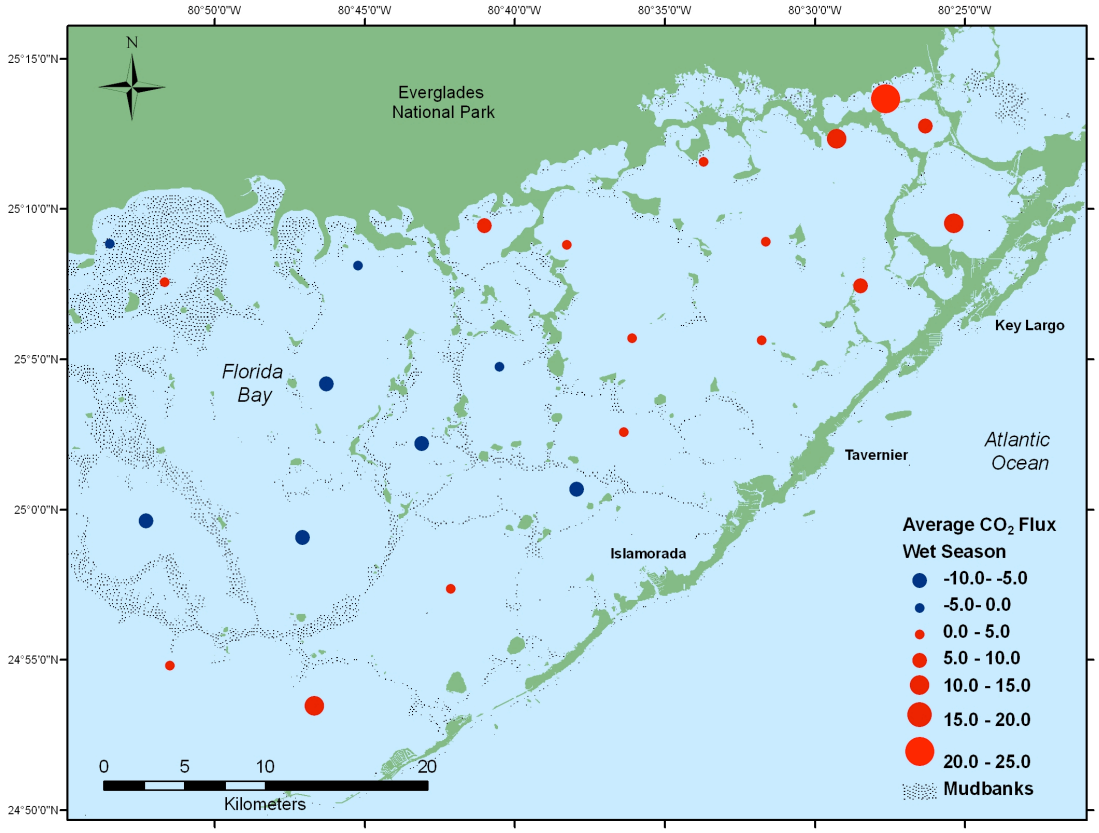

Figure 13. Average CO_2 flux at each sampling location for all measurements collected during the wet season (May through October).

In a study examining the diurnal variation in carbonate system parameters, Yates et al. (2007) reported an 80% diurnal range and a 136% 3-day range in pCO_2 values collected from a sampling location in Florida Bay near the transition zone of the east, central, and south regions. Although all of the data collected during my study were obtained during daylight hours, diurnal variability has the potential to create a significant bias in temporal data.

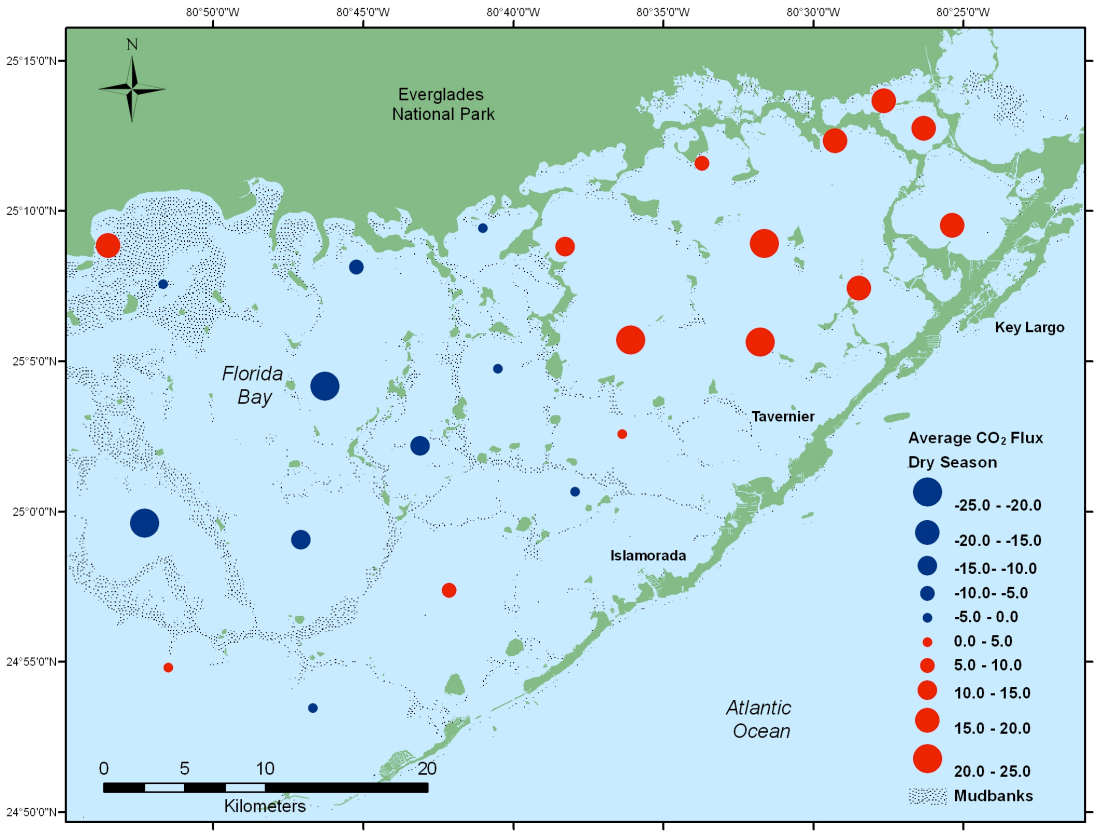

Figure 14. Average CO_2 flux at each sampling location for all measurements collected during the dry season (November through April).

Characterization of the Carbonate System: DIC –TA Relationships

Water samples collected during the final four sampling trips (April 2002 to April 2003) were used to investigate the carbonate system in Florida Bay and relate flux measurement results to pCO_2 differences between water and air. Appendix IV lists the results of the alkalinity and dissolved inorganic carbon analyses conducted on seawater samples collected at each sampling site. DIC and TA were used to calculate pCO_2, pH and saturation state for all collected samples.

DIC and TA were strongly correlated ($R^2 = 0.94$) over the entire sampling period (Figure 15 and equation 9).

$$DIC = 1.17 \times TA - 816.63 \quad \text{Eq. 9}$$

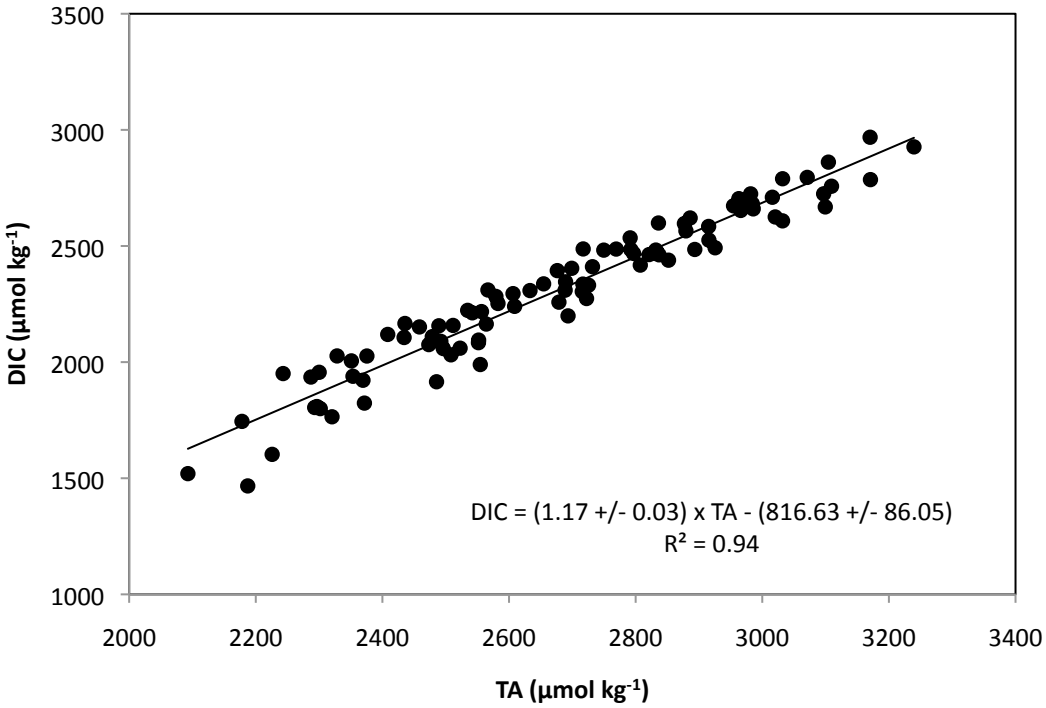

Figure 15. Linear relationship between measured total alkalinity and dissolved inorganic carbon collected during the final four sampling trips.

A similar plot of normalized DIC (NDIC = DIC x 35/S) vs. normalized TA (NTA = TA x 35/S) (Figure 16 and equation 10) exhibited an even more coherent relationship ($R^2 = 0.99$).

$$NDIC = 0.993 \times NTA - 412.84 \quad \text{Eq. 10.}$$

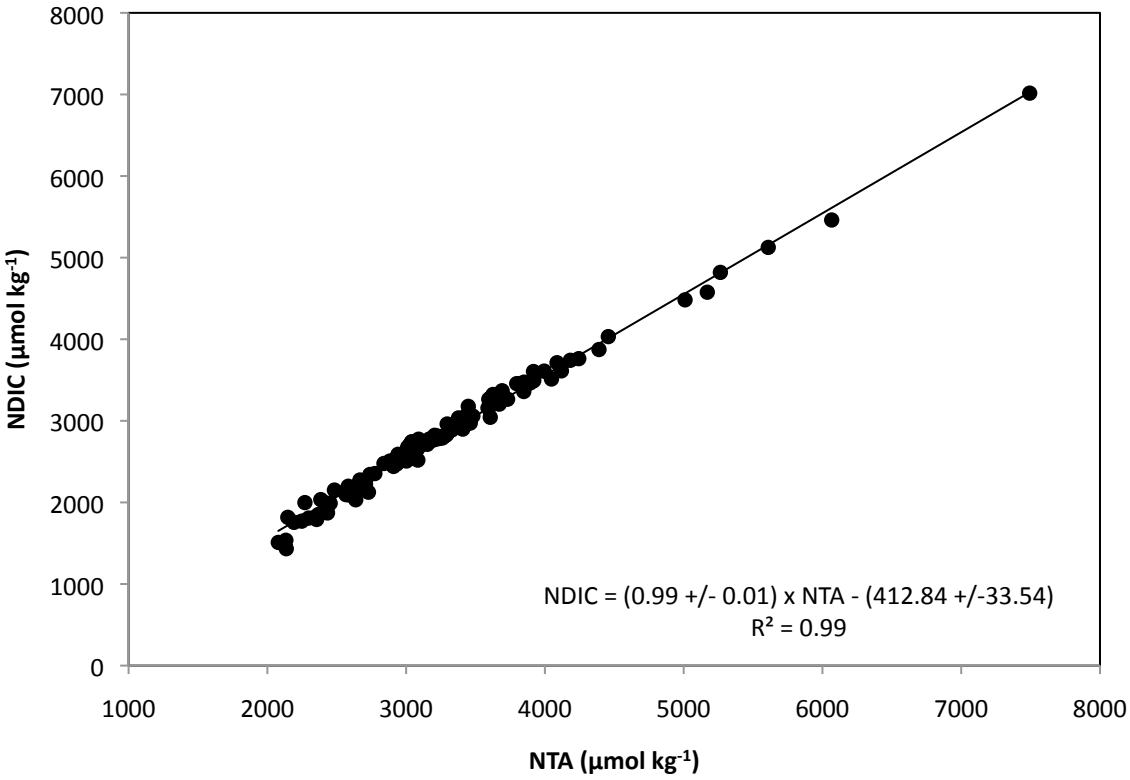

Figure 16. Linear relationship between normalized total alkalinity and normalized dissolved inorganic carbon collected during the final four sampling trips.

The improved coherence seen in Figure 16 relative to Figure 15 can be attributed to the strong influence of salinity on the relationship between DIC and TA. Equation 10 can be rewritten in the following form:

$$DIC = 0.993\ TA - 412.8\ (S/35) \qquad \text{Eq. 11.}$$

Equation 11 is consistent with mixing of seawater and Everglades freshwater in which the total alkalinity exceeds DIC to an extent that is directly proportional to salinity. The coherence of Eq. 11 relative to Eq. 9 in descriptions of DIC – TA relationships can be examined by comparing direct observations of DIC with predictions based alternatively on Eq. 9 and Eq. 11:

$$\text{DIC (observed)}_i - \text{DIC (calculated – Eq. 9)}_i = \Delta(\text{DIC})_i \qquad \text{Eq. 12a.}$$

$$\text{DIC (observed)}_i - \text{DIC (calculated – Eq. 11)}_i = \Delta(\text{DIC})_i \qquad \text{Eq. 12b.}$$

For the data shown in Figure 15, the sum of squares of residuals ($\sum_i \Delta(\text{DIC})_i$) obtained using Eq. 12a is 635,410, and the sum of squares of residuals obtained using Eq. 12b is approximately 19% smaller ($\sum_i \Delta(\text{DIC})_i$ = 516,091). Thus, CO_2 system characteristics in Florida Bay, including patterns of CO_2 fluxes are strongly related to mixing of water masses. With increasing salinity, the TA/DIC ratio increases, resulting in higher pH, lower pCO_2 and lower CO_2 flux into the atmosphere.

Relationship Between Measured CO_2 Flux and Calculated ΔpCO_2

Since the dependence of K_o on temperature and ionic strength is known, as shown in equation 3 the observed flux measurements can be expressed in the following form:

$$F = k([CO_2]_{(water)} - [CO_2]_{(air)}) = k\,(K_o\,(pCO_{2(water)} - pCO_{2(air)}) \qquad \text{Eq. 13}$$

Figure 17 shows CO_2 fluxes (F) plotted as a function of $(pCO_{2(water)} - pCO_{2(air)})$. A fit of flux vs. ΔpCO_2 of the form $F_o = S(pCO_{2(water)} - pCO_{2(air)}) + I_o$ produces an intercept (I_o) that is statistically indistinguishable from zero (I_o = 0.238 +/- 0.679). As such, the data shown in Figure 17 were fit assuming a zero intercept (Figure 18). The best-fit result using equation 13 is given as:

$$F_0 = \{(74 \pm 4)\ \text{mol atm}^{-1}\ \text{m}^{-2}\ \text{d}^{-1}\}(pCO_{2(water)} - pCO_{2(air)}). \qquad \text{Eq. 14}$$

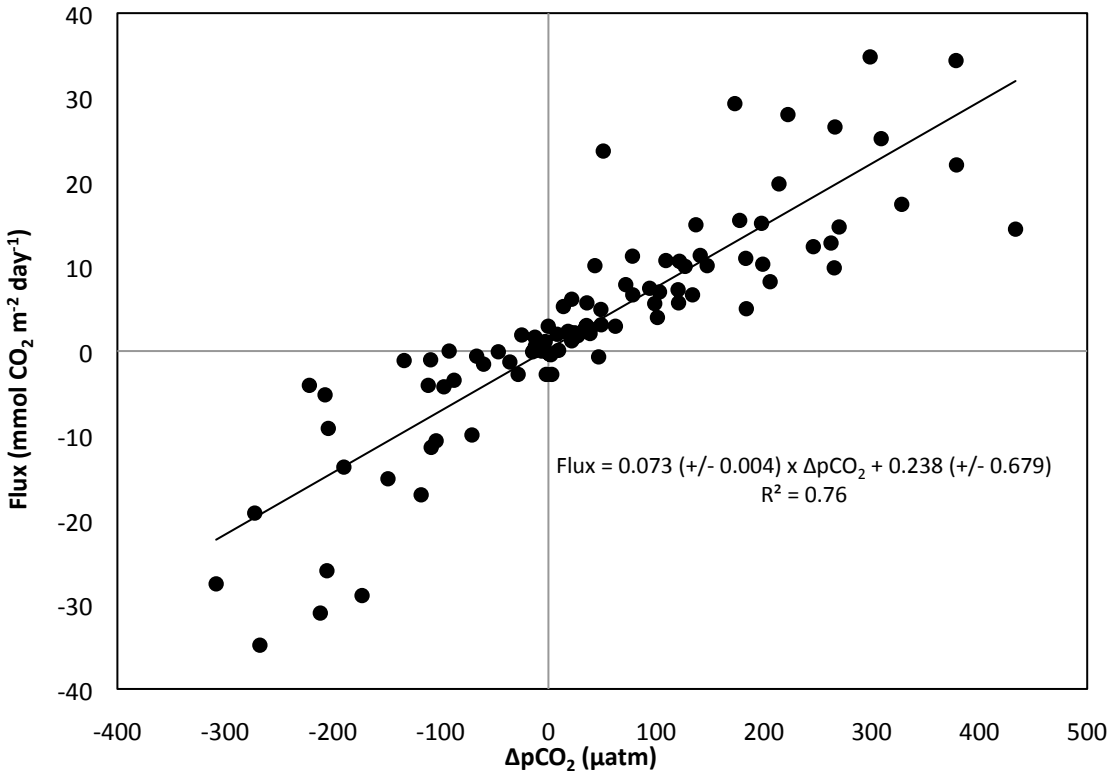

Figure 17. CO_2 flux (mmol m^{-2} day^{-1}) as a function of ΔpCO_2 (µatm).

It has been shown that changes in k due to temperature are nearly compensated by the temperature dependence of K_0 such that the product of kK_0 is nearly temperature independent (Wanninkhof, 1992). Using the solubility of CO_2 in seawater at 20˚ C (K_o = 33.22 mol m^{-3} atm^{-1}), the gas transfer velocity (k) is then given as k = {(74 ± 4)/(33.22)} m d^{-1} = 9.3 ± 0.5 cm h^{-1}. This value is in good agreement with the k_{660} value of McGillis et al. (2004) for zero wind velocity (i.e., $k_{660} = 8.2 + 0.014\ u_{10}^3$, where u_{10} denotes wind velocity 10 m above sea level).

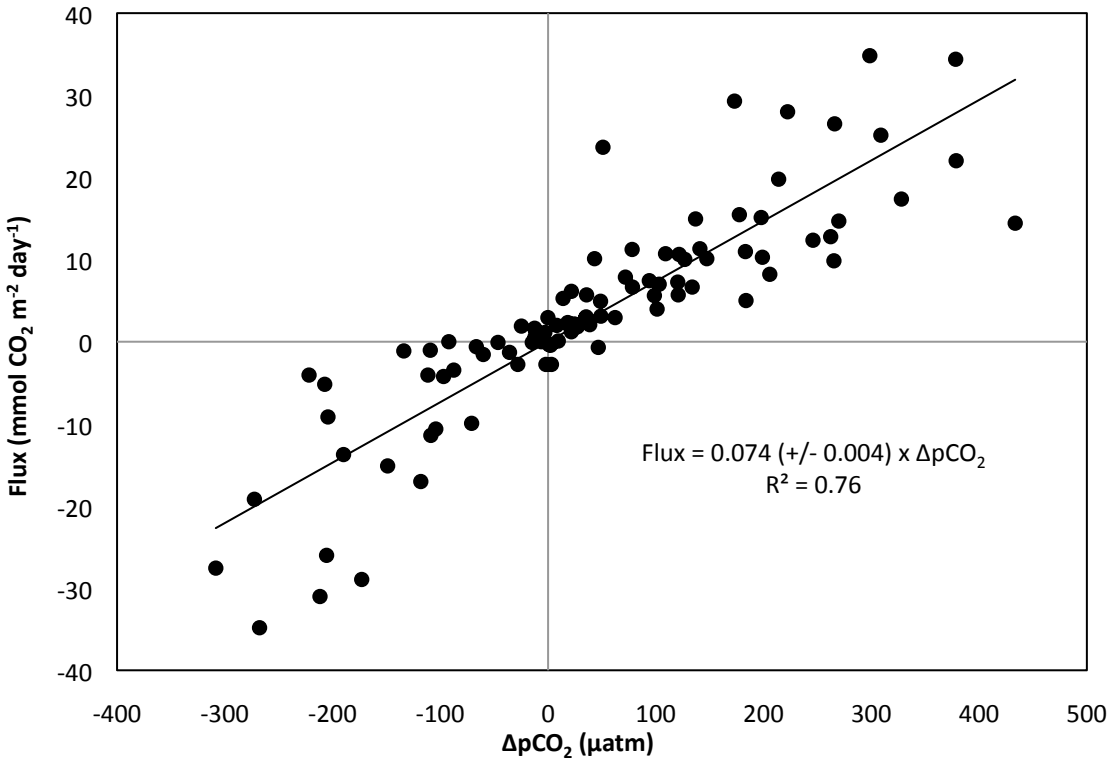

Figure 18. CO_2 flux (mmol m^{-2} day^{-1}) as a function of ΔpCO_2 (µatm).

Predicting ΔpCO_2

The regression for the flux measurements and the ΔpCO_2 given in Equation 14 provides a means of predicting ΔpCO_2 using floating chamber measurements of CO_2 fluxes at zero wind velocity (F_0). Assuming that flux measurements obtained using closed chambers during my study show little or no influence from ambient wind speed (i.e., wind speed inside the chamber is zero), equation 14 can be restated as

$$\Delta pCO_2 \text{ (atm)} = F_0 \text{ (mol m}^{-2} \text{ d}^{-1}\text{)} / 74 \text{ (mol atm}^{-1} \text{ m}^{-2} \text{ d}^{-1}\text{)} \quad \text{Eq. 15}$$

where F_0 is a flux at zero wind speed in a floating chamber.

During the GasEx-2001 cruise McGillis et al. (2004) used an eddy correlation method and found that the influence of wind speed on gas transfer velocity could be described with a cubic relationship of the form

$$k = 8.2 + 0.014\ u_{10}^{3}(Sc/660)^{-n} \qquad \text{Eq. 16}$$

where u_{10} is the wind speed at 10 m height, Sc is the Schmidt number for CO_2, 660 is the Schmidt number of CO_2 in seawater at 20˚C and n is a hydrodynamic variable adjusted for flow conditions; typically assigned a value n = 2/3 for smooth conditions and n = 1/2 for wavy conditions. Equations 13, 15 and 16 were used in conjunction with the F_0 data obtained throughout this investigation (i.e. the final column of Tables 1 through 9, Appendix III), to predict average CO_2 fluxes (F) at ambient wind speeds over the 25-month period of my investigation:

Wind speed data, collected at a height of 7 meters, were taken from the Coastal-Marine Automated Network (C-MAN) station located off of Long Key, Florida (24.843˚ N 80.862˚ W) and adjusted to a height of 10 meters using the power-law wind profile relationship of Hsu et al. (1994) with an exponent $P = 0.11$.

$$u_2/u_1 = (z_2/z_1)^{P} \qquad \text{Eq. 17}$$

where u_2 is the wind speed at height z_2, u_1 is the known wind speed at height z_1, and P is a function of both atmospheric stability and surface roughness (Hsu et al. 1994).

By using equation 15 calculations of ΔpCO_2, gas transfer velocities (k) calculated via equation 16, and the flux relationship given as equation 13, my floating chamber F_0 measurements were used to predict flux values appropriate to the natural environment of Florida Bay. The results shown in Figure 19, and listed in Table 1, are very similar to the results presented in Figure 3, indicating that for the generally low wind velocities

observed during the course of my investigation, the wind velocity term in equation 16 contributes very little to Florida Bay CO_2 fluxes. The average yearly CO_2 flux for the entire Florida Bay study area was 3.9 mmol CO_2 m^{-2} d^{-1} .

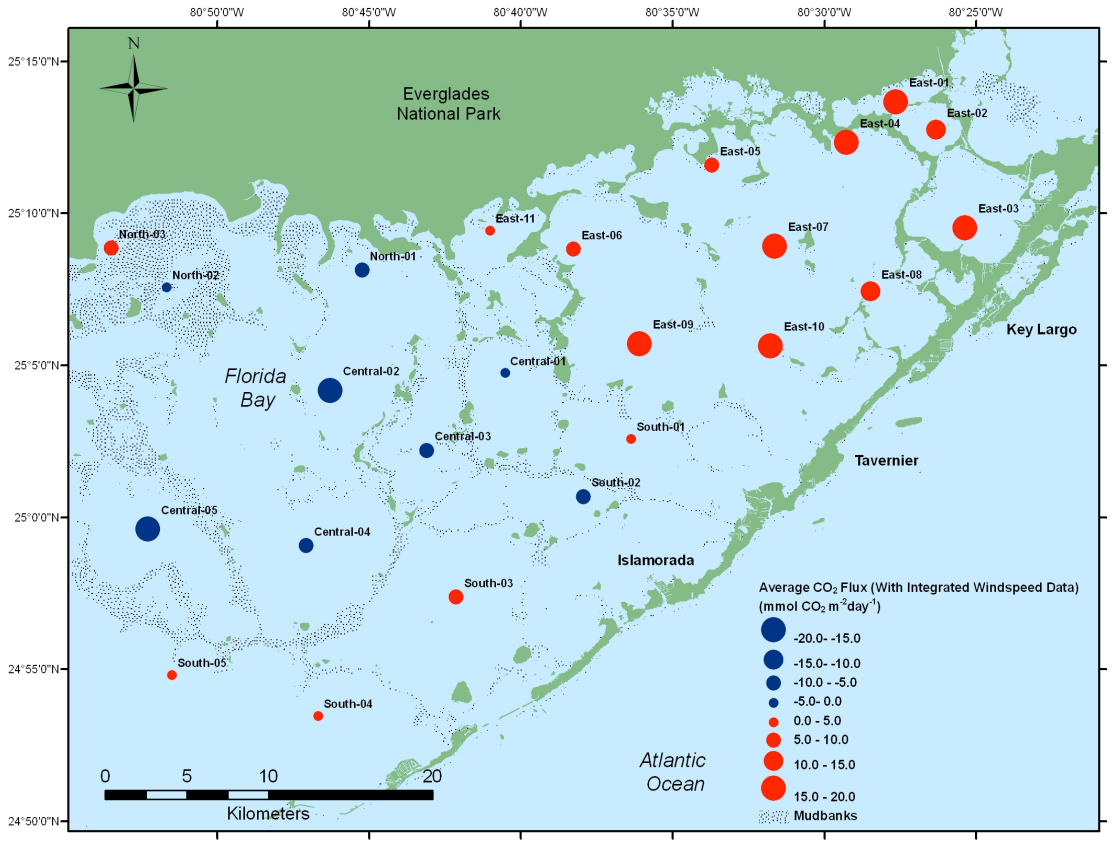

Figure 19. Average CO_2 fluxes obtained using equations 13, 15 and 16 at each sampling location for all F_0 measurements obtained during this study.

Table 1. Average CO_2 fluxes shown in Figure 19.

Station	CO_2 flux (mmol m^{-2} d^{-1})	Station	CO_2 flux (mmol m^{-2} d^{-1})
East-01	19.2	North-02	-2.7
East-02	13.7	North-03	9.6
East-03	18.7	Central-01	-3.5
East-04	15.2	Central-02	-18.5
East-05	5.8	Central-03	-9.7
East-06	9.3	Central-04	-8.7
East-07	16.6	Central-05	-19.3
East-08	14.3	South-01	3.5
East-09	17.3	South-02	-5.5
East-10	17.3	South-03	6.8
East-11	1.3	South-04	3.7
North-01	-7.3	South-05	0.9

Conclusions

A floating chamber was used during this study to measure CO_2 flux across the air-water interface at zero wind velocity. Measurements of dissolved inorganic carbon and total alkalinity obtained concurrently with chamber measurements of CO_2 flux allow calculation of ΔpCO_2 from flux measurements obtained at zero wind velocity. Floating chamber measurements of ΔpCO_2 were subsequently coupled with wind speed data to provide a simple yet reliable means of predicting absolute flux values.

Biogeochemical conditions in Florida Bay are highly variable due to wide variations in fresh water input and the influence of topography on water circulation. Freshwater input in Florida Bay from land runoff is focused in the eastern portion of the bay, while the central portion is dominated by precipitation and dissolution. Mudbanks in Florida Bay are prominent topographical features that restrict circulation and play an important role, along with tidal exchange, in controlling the chemistry of the bay. Shallow water depths along with an abundance of both planktonic and benthic flora and fauna may also have an important influence on carbon fluxes within the bay.

Four distinct zones of Florida Bay were identified in this study. The eastern portion of the bay receives the majority of freshwater input in the form of sheet flow from Taylor Slough. This area is typical of estuarine waters and, during the course of my study, exhibited a net CO_2 flux from water to air. The central portion of the bay,

comprised of a number of shallow semi-isolated basins that limited exchange with the bulk of the bay waters, exhibited periods of hypersalinity and typically served as a sink of atmosphere CO_2 in the course of my study. Low pCO_2 in the central portion of the bay may be due in part to high levels of both benthic and pelagic primary productivity possibly combined with carbonate sediment dissolution. The northern region of the bay and the eastern portion of the bay both have a mangrove fringe, but the northern bay has a much larger CO_2 flux variability. Shallow water and benthic and planktonic community structure may impact the chemistry in this area along with a comparatively diminished flow of freshwater from the land. The southern portion of the bay is exposed to extensive tidal exchange with the waters of the Atlantic Ocean and exhibits modest variability in CO_2 flux.

Variability in flux measurements over the entire course of this study showed significant patterns of spatial and temporal variability, especially in the eastern and central regions. Interestingly, the largest flux values, both influx in the central region and efflux in the eastern region, were recorded during the drier winter months. This may suggest that longer residence times, due to diminished freshwater input from both runoff and precipitation, has a major impact on bay water chemistry. However, it seems likely that both photosynthesis/respiration and calcification/dissolution are also important.

References

Borges, A. V., 2005. Do we have enough pieces of the jigsaw to integrate CO_2 fluxes in the coastal ocean? Estuaries, 28(1), 3-27.

Borges, A. V., B. Delille, and M. Frankignoulle, 2005. Budgeting sinks and sources of CO_2 in the coastal ocean: Diversity of ecosystem counts. Geophysical Research Letters, 32, L14601.

Bosence, D., 1989a. Biogenic carbonate production in Florida Bay. Bulletin of Marine Science, 44(1), 419-433.

Bosence, D, 1989b. Surface sublittloral sediments of Florida Bay. Bulletin of Marine Science, 44(1), 434-453.

Boyer, J. N., J. W. Fourqurean and R. D. Jones, 1997. Spatial characterization of water quality in Florida Bay and Whitewater Bay by multivariate analyses: Zones of similar influence. Estuaries, 20(4), 743-758.

Broecker, H. C., J. Peterman, and W. Siems, 1978. The influence of wind on CO_2 exchange in a wind-wave tunnel, including the effects of mono layers. Journal of Marine Research, 36, 595-610.

Broecker, W. S., J. R. Ledwell, T. Takahashi, L. M. R. Weiss, L. Memery, T.-H. Peng, B. Jähne, and K. O. Münnich, 1986. Isotopic versus micrometeorologic ocean CO_2 fluxes: A serious conflict. Journal of Geophysical Research, 91, 10,517-10,527.

Broecker, W. S., T.-H. Peng, G. Östlund and M. Stuiver, 1985. The distribution of bomb radiocarbon in the ocean. Journal of Geophysical Research, 99, 6953-6970.

Broecker, W. S., S. Sutherland, W. Smethie, T.-H. Peng, and G. Östlund, 1995. Oceanic radiocarbon: separation of the natural and bomb components. Global Biogeochemical Cycles, 9, 263-288.

Cai, W.-J. and Y. Wang, 1998. The chemistry, fluxes, and sources of carbon dioxide in the estuarine waters of the Satilla and Altamaha Rivers, Georgia. Limnology and Oceanography, 43(4), 657-668.

Cember, R., 1989. Bomb radiocarbon in the Red Sea: A medium-scale gas exchange experiment. Journal of Geophysical Research, 94, 2111-2123.

Costello, T. J., D. M. Allen, and J. H. Hudson, 1986. Distribution, seasonal abundance and ecology of juvenile northern pink shrimp, *Penaeus duorarum*, in the Florida Bay area. NOAA Tech. Mem., NMFS-SEFC-161, 1-84.

Crusius, J. and R. Wanninkhof, 2003. Gas transfer velocities measured at low speed over a lake. Limnology and Oceanography, 48(3), 1010-1017.

Denman, K. L., G. Brasseur, A. Chidthaisong, P. Ciais, P. M. Cox, R. E. Dickinson, D. Hauglustaine, C. Heinze, E. Holland, D. Jacob, U. Lohmann, S. Ramachandran, P. L. da Silva Dias, S. C. Wofsy, and X. Zhang, 2007. Couplings between changes in the climate system and biogeochemistry, 499-587. *In* Soloman, S., D. Qin, M. Manning, Z. Chen, M. Marquis, K. B. Averyt, M. Tignor, and H. L. Miller (eds.), Climate Change 2007: The Physical Science Basis. Contributions of Working Group I to the Fourth Assessment Report of the Intergovernmental Panel on Climate Change. Cambridge University Press, Cambridge, UK and New York, NY.

Dickson, A. G., 1990. Standard potential of the reaction: $AgCl(s) + ½ H_2(g) = Ag(s) + HCl(aq)$, and the standard acidity constant of the ion HSO_4^- in synthetic seawater from 273.15 to 318.15 K. Journal of Chemical Thermodynamics, 22, 113-127.
Dickson, A. G., 1981. An exact definition of total alkalinity and a procedure for the estimation of alkalinity and total inorganic carbon from the titration data. Deep Sea Research A, 28(6), 609-623.

Dickson, A. G., and F. J. Millero, 1987. A comparison of the equilibrium constants for the dissociation of carbonic acid in seawater media. Deep-Sea Research, 34, 1733-1743.

DOE, 1994. Handbook of methods for the analysis of the various parameters of the carbon dioxide system in sea water; version 2. A. G. Dickson and C. Goyet, eds. ORNL/CDIAC-74.

Duever, M. J., J. F. Meeder, L. C. Meeder, and J. M. McCollom, 1994. The climate of South Florida and its role in shaping the Everglades ecosystem, 225-248. *In* S. M. Davis and J. C. Ogden (eds.), Everglades: The Ecosystem and Its Restoration. St. Lucie Press, Delray Beach, FL.

Enos, P. and R. D. Perkins, 1979. Evolution of Florida Bay from island stratigraphy. Geological Society of America Bulletin, 90, 59-83.

Etheridge, D. M., L. P. Steele, R. L. Lagenfelds, R. J. Francey, J.-M. Barnola and V. I. Morgan, 1996. Natural and anthropogenic changes in atmospheric CO_2 over the last 1000 years from the air in Antarctic ice and firn. Journal of Geophysical Research, 101(D2), 4115-4128.

Fourqurean, J. W., R. D. Jones, and J. C. Zieman, 1993. Processes influencing water column nutrient characteristics and phosphorous limitation of phytoplankton biomass in Florida Bay, FL, USA: Inferences from spatial distributions. Estuarine, Coastal and Shelf Science, 36, 295-314.

Fourqurean, J. W., and M. B. Robblee, 1999. Florida Bay: A history of recent ecological changes. Estuaries, 22, 345-357.

Frankignoulle, M., 1988. Field measurements of air-sea CO_2 exchange. Limnology and Oceanography, 33(3), 313-322.

Frankignoulle, M., G. Abril, A. Borges, I. Bourge, C. Canon, B. Delille, E. Libert, and J.-M. Théate, 1998. Carbon dioxide emission from European estuaries. Science, 282, 434-436.

Hittle, C., 2001. Quantity, timing, and distribution of freshwater flows into northeastern Florida Bay. 2001 Florida Bay Science Conference (abs.), Key Largo, FL.

Ho, D. T., P. Schlosser, and P. M. Orton, In Press. On factors controlling air-water gas exchange in a large tidal river. Estuaries and Coasts.

Homquist, J. G., G. V. N. Powell, and S. M. Sogard, 1989. Sediment, water level and water temperature characteristics of Florida Bay's grass-covered mud banks. Bulletin of Marine Science, 44(1), 348-364.

Houghton, R. A., 2003. Revised estimates of the annual net flux of carbon to the atmosphere from changes in land use and land management 1850-2000. Tellus, 55B(2), 378-390.

Hsu, S. A., E. A. Meindl, and D. B. Gilhousen, 1994. Determining the power-law wind-profile exponent under near-neutral stability conditions at sea. Journal of Applied Meteorology, 33, 757-765.

Jähne, B., W. Huber, A. Dutzi, T. Wais, and J. Ilmberger, 1984. Wind/wave tunnel experiment on the Schmidt number—And wave field dependence of air/water gas exchange, 303-309. *In* W. Brutsaert and G. H. Jirka (eds.), Gas Transfer at Water Surfaces. Reidel Publishing Co., Dordrecht, The Netherlands.

Jiang, L.-Q., W.-J. Cai, and Y. Wang, 2008. A comparative study of carbon dioxide degassing in river- and marine-dominated estuaries. Limnology and Oceanography, 53(6), 2603-2615.

Keeling, C. D. and T. P. Whorf, 2005. Atmospheric CO_2 records from sites in the SIO sampling network. *In* Trends: A Compendium of Data on Global Change. Carbon Dioxide Information Analysis Center, Oak Ridge National Laboratory, U.S. Department of Energy, Oak Ridge, TN.

Kelble, C. R., E. M. Johns, W. K. Nuttle, T. N. Lee, R. H. Smith, and P. B. Ortner, 2007. Salinity patterns of Florida Bay. Estuarine, Coastal and Shelf Science, 71, 318-334.

Kremer, J. N., S. W. Nixon, B. Buckley, and P. Roques, 2003. Technical note: Conditions for using the floating chamber method to estimate air-water gas exchange. Estuaries, 26(4a), 985-990.

Le Quéré, C., O. Aumont, L. Bopp, P. Bousquet, P. Ciais, R. Francey, M. Heimann, C. D. Keeling, R. F. Keeling, H. Kheshgi, P. Peylin, S. C. Piper, I. C. Prentice, and P. J. Rayner, 2003. Two decades of ocean CO_2 sink and variability. Tellus B, 55, 649–656.

Le Treut, H., R. Sommerville, U. Cubasch, Y. Ding, C. Mauritzen, A. Mokssit, T. Peterson, and M. Prather, 2007. Historical overview of climate change science, 93-127. *In* Soloman, S., D. Qin, M. Manning, Z. Chen, M. Marquis, K. B. Averyt, M. Tignor, and H. L. Miller (eds.), Climate Change 2007: The Physical Science Basis. Contributions of Working Group I to the Fourth Assessment Report of the Intergovernmental Panel on Climate Change. Cambridge University Press, Cambridge, UK and New York, NY.

Lee, T. N., E. Johns, N. Melo, R. H. Smith, P. Ortner, and D. Smith, 2006. On Florida Bay hypersalinity and water exchange. Bulletin of Marine Science, 79(2), 301-327.

Lewis, E., and D. W. R. Wallace, 1998. Program developed for CO_2 system calculations. ORNL/CDIAC-105. Carbon Dioxide Information Analysis Center, Oak Ridge National Laboratory, U.S. Department of Energy, Oak Ridge, Tennessee.

Liss, P. S. and L. Merlivat, 1986. Air-sea gas exchange rates: introduction and synthesis. *In* P. Baut-Ménard (ed.), The Role of Air-Sea Exchange in Geochemical Cycling. Reidel, Boston, MA.

MacFarling Meure, C. D. Etheridge, C. Trudinger, P. Steele, R. Lagenfelds, T. van Ommen, A. Smith and J. Elkins, 2006. Law dome CO_2, CH_4 and N_2O ice core records extended to 2000 years BP. Geophysical Research Letters, 33, L14810.

Marino, R. and R. W. Howarth, 1993. Atmospheric oxygen exchange in the Hudson River: Dome measurements and comparison with other natural waters. Estuaries, 16(3a), 433-445.

Marland, G., T. A. Boden, and R. J. Andres, 2006. Global, regional, and national CO_2 emissions. *In* Trends: A Compendium of Data on Global Change. Carbon Dioxide Information Analysis Center, Oak Ridge National Laboratory, U.S. Department of Energy, Oak Ridge, TN.

McGillis, W. R., J. B. Edson, C. J. Zappa, J. D. Ware, S. P. McKenna, E. A. Terray, J. E. Hare, C. W. Fairall, W. Drennan, M. Donelan, M. D. DeGrandpre, R. Wanninkhof, and R. A. Feely, 2004. Air-sea CO_2 exchange in the equatorial Pacific. Journal of Geophysical Research, 109(C08S02), ?.

McGillis, W. R., and R. Wanninkhof , 2006. Aqueous CO_2 gradients for air-sea flux estimates. Marine Chemistry, 98, 100-108.

McIvor, C. C., J. A. Ley, and R. D. Bjork, 1994. Changes in freshwater inflow from the Everglades to Florida Bay including effects on biota and biotic processes: a review, 117-146. *In* J. Ogden and S. Davis (eds.), Everglades: The Ecosystem and Its Restoration. St. Lucie Press, Delray Beach, FL.

Meehl, G. A., T. F. Stocker, W. D. Collins, P. Friedlingstein, A. T. Gaye, J. M. Gregory, A. Kitoh, R. Knutti, J. M. Murphy, A. Noda, S. C. B. Raper, I. G. Waterson, A. J. Weaver, and Z.-C. Zhao, 2007. Global climate projections, 747-845. *In* S. Soloman, D. Qin, M. Manning, Z. Chen, M. Marquis, K. B. Averyt, M. Tignor, and H. L. Miller (eds.), Climate Change 2007: The Physical Science Basis. Contributions of Working Group I to the Fourth Assessment Report of the Intergovernmental Panel on Climate Change. Cambridge University Press, Cambridge, UK and New York, NY.

Mehrbach, C., C. H. Culberson, J. E. Hawley, and R. M. Pytkowicz, 1973. Measurement of the apparent dissociation constants of carbonic acid in seawater at atmospheric pressure. Limnology and Oceanography, 18, 897-907.

Millero, F. J., 2007. The marine inorganic carbon cycle. Chemical Reviews, 107, 308-341.

Millero, F. J., W. T. Hisock, F. Huang, M. Roche, and J. Z. Zhang, 2001. Seasonal variation in the carbonate system in Florida Bay. Bulletin of Marine Science, 68(1), 101-123.

Morse, J. W. and F. T. Mackenzie, 1990. Geochemistry of Sedimentary Carbonates. Elsevier, Amsterdam, 707 pp.

Mukhopadhyay, S. K., H. Biswas, T. K. De, S. Sen, and T. K. Jana, 2002. Seasonal effects on the air-water carbon dioxide exchange in the Hooghly estuary, NE coast of Bay of Bengal, India. Journal of Environmental Monitoring, 4, 549-552.

Neftel, A., E. Moor, H. Oeschger and B. Stauffer, 1985. Evidence from polar ice cores for the increase in atmospheric CO_2 in the past two centuries. Nature, 315, 45-47.

Nuttle, W. K., J. W. Fourqurean, B. J. Cosby, J. C. Zieman, and M. B. Robblee, 2000. Influence of net freshwater supply on salinity in Florida Bay. Water Resources Research, 36, 1805-1822.

Obeysekera, J., J. Browder, L. Hornung, and M. A. Harwell, 1999. The natural South Florida system I: Climate, geology, and hydrology. Urban Ecosystems, 3, 223-244.

Phlips, E. J., S. Badyluk, and T. C. Lynch, 1999. Blooms of the picoplanktonic cyanobacterium *Synechococcus* in Florida Bay, a subtropical inner shelf lagoon. Limnology and Oceanography, 44, 1166-1175.

Pilson, M.E.Q., 1998. An Introduction to the Chemistry of the Sea. Prentice Hall, Upper Saddle River, NJ, 431 pp.

Powell, G. V. N., W. J. Kenworthy, and J. W. Fourqurean, 1989. Experimental evidence for nutrient limitation of seagrass growth in a tropical estuary with restricted circulation. Bulletin of Marine Science, 44(1), 324-340.

Prager, E. J. and R. B. Halley, 1997. Florida Bay bottom types. U. S. Geological Survey open file report 97-526.

Riley, J. P., and M. Tongudai, 1967. The major cation/chlorinity ratios in sea water. Chemical Geology, 2, 263-269.

Schomer, N. S. and R. D. Drew, 1982. An ecological characterization of the Lower Everglades, Florida Bay and the Florida Keys. US Fish and Wildlife Service, Office of Biological Services, Washington, D.C. FWS/OBS 82/58.1.

Smith, N. P., 1997. An introduction to the tides of Florida Bay. Florida Scientist, 60(1), 53-67.

Smith, S. V., and J. T. Hollibaugh, 1993. Coastal metabolism and the oceanic organic carbon cycle. Reviews of Geophysics, 31, 75-89.

Swart, P. K. and R. Price, 2002. Origin of salinity variations in Florida Bay. Limnology and Oceanography, 47(4), 1234-1241.

Turney, W. J. and B. F. Perkins, 1972. Molluscan distribution in Florida Bay. Sedimenta III. Rosenstiel School of Marine and Atmospheric Sciences, University of Miami, FL.

Wanless, H. R., and M. G. Tagett, 1989. Origin, growth and evolution of carbonate mudbanks in Florida Bay. Bulletin of Marine Science, 44, 454-489.

Wanninkhof, R., 1992. Relationship between wind speed and gas exchange over the ocean. Journal of Geophysical Research, 97(C5), 7373-7382.

Wanninkhof, R., W. E. Asher, D. T. Ho, C. Sweeney, and W. R. McGillis, 2009. Advances in quantifying air-sea gas exchange and environmental forcing. Annual Review of Marine Science, 1, 213-244.

Wanninkhof, R., J. R. Ledwell, and W. S. Broecker, 1985. Gas exchange-wind speed relationship measured with sulfur hexafluoride on a lake. Science, 227, 1224-1226.

Yao, W. and R. H. Byrne, 1998. Simplified seawater alkalinity analysis - application to the potentiometric titration of the total alkalinity and carbonate content in sea water. Deep Sea Research I, 45(8), 1383-1392.

Yates, K. K., C. DuFore, N. Smiley, C. Jackson, and R. B. Halley, 2007. Diurnal variation of oxygen and carbonate system parameters in Tampa Bay and Florida Bay. Marine Chemistry, 104, 110-124.

Zieman, J. C., J. W. Fourquerean, and R. L. Iverson, 1989. Distribution, abundance and productivity of seagrasses and macroalgae in Florida Bay. Bulletin of Marine Science, 44(1), 292-311.

Bibliography

Borges, A. V., B. Delille and L.-S. Schiettecatte, 2004. Gas transfer velocities of CO_2 in three European estuaries (Randers Fjord, Scheldt, and Thames). Limnology and Oceanography, 49(5), 1630-1641.

Borges, A. V., S. Djenidi, G. Lacroix, J. Théata, B. Delille, and M. Frankignoulle, 2003. Atmospheric CO_2 flux from mangrove surrounding waters. Geophysical Research Letters, 30(11), 1558.

Broecker, W. S. and T.-H. Peng, 1984. Gas exchange measurements in natural systems, 479-495. *In* W. Brutsaert and G. H. Jirka (eds.), Gas Transfer at Water Surfaces. Reidel Publishing Co., Dordrecht, The Netherlands.

Carini, S., N. Weston, C. Hopkinson, J. Tucker. A. Giblin, and J. Vallino, 1996. Gas exchange rates in the Parker River estuary, Massachusetts. Biological Bulletin, 191, 333-334.

Cerco, C. F., 1989. Estimating estuarine reaeration rates. Journal of Environmental Engineering, 115(5), 1066-1070.

Cole, J. J. and N. F. Caraco, 1998. Atmospheric exchange of carbon dioxide in a low-wind oligotrophic lake measured by the addition of SF_6. Limnology and Oceanography, 43(4), 647-656.

Dickson, A. G., J. D. Afghan, and G. C. Anderson, 2003. Reference materials for Oceanic CO_2 analysis: a method for the certification of total alkalinity. Marine Chemistry, 80, 185-197.

Dickson, A. G. and J. P. Riley, 1978. The effect of analytical error on the evaluation of the components of the aquatic carbon-dioxide system. Marine Chemistry, 6, 77-85.

Emerson, S., 1975. Chemically enhanced CO_2 gas exchange in a eutrophic lake: A general model. Limnology and Oceanography, 20(5), 743-753.

Enos, P., 1989. Islands in the bay – A key habitat of Florida Bay. Bulletin of Marine Science, 44(1), 365-386.

Frankignoulle, M., R. Biondo, J.-M. Théate, and A. V. Borges, 2003. Carbon dioxide daily variations and atmospheric fluxes over the open waters of the Great Bahama Bank and Norman's Pond using a novel autonomous measuring system. Caribbean Journal of Science, 39(3), 257-264.

Frankignoulle, M. and A. Disteche, 1987. Study of the transmission of the diurnal CO_2 concentration changes observed above a *Posidonia* seagrass bed: a method to determine the turbulent diffusion coefficient in an 8-m water column. Continental Shelf Research, 7(1), 67-76.

Hartman, B. and D. E. Hammond, 1984. Gas exchange rates across the sediment-water and air-water interfaces in south San Francisco Bay. Journal of Geophysical Research, 89(C3), 3593-3603.

Ho, D. T., C. J. Zappa, W. R. McGillis, L. F. Bliven, B. Ward, J. W. H. Dacey, P. Schlosser, and M. B. Hendricks, 2004. Influence of rain on air-sea gas exchange: Lessons from a model ocean. Journal of Geophysical Research, 109, C08S18.

Jähne, B., K. O. Munnich, R. Bosinger, A. Dutzi, W. Huber, and P. Libner, 1987. On parameters influencing air-water gas exchange. Journal of Geophysical Research, 92, 1937-1949.

Keeling, C. D., 1960. The concentration and isotopic abundances of carbon dioxide in the atmosphere. Tellus, 12, 200-203.

Liss, P. S., 1983. Gas transfer: experiments and geochemical implications, 241-299. *In* P. S. Liss and W. G. Slinn (eds.), Air-Sea Exchange of Gases and Particles. Reidel, Boston, MA.

MacIntyre, S., R. Wanninkhof, and J. P. Chanton, 1995. Trace gas exchange across the air-water interface in freshwater and coastal marine environments, 52-97. *In* P. A. Matson and R. C. Harris (eds.), Biogenic Trace Gases: Measuring Emissions from Soil and Water. Blackwell Science, Cambridge, MA.

Matthews, C. J. D., V. L. St. Louis, and R. H. Hesslein, 2003. Comparison of three techniques used to measure diffusive gas exchange from sheltered aquatic surfaces. Environ. Sci. Technol., 37, 772-780.

Millero, F. J., R. H. Byrne, R. Wanninkhof, R. Feely, T. Clayton, P. Murphy and M. F. Lamb, 1993a. The internal consistency of CO_2 measurements in the Equatorial Pacific. Marine Chemistry, 44, 269-280.

Millero, F. J., J.-Z. Zhang, K. Lee, and D. M. Campbell, 1993b. Titration alkalinity of seawater. Marine Chemistry, 44, 153-165.

Mucci, A., 1983. The solubility of calcite and aragonite in seawater at various salinities, temperatures, and one atmosphere total pressure. American Journal of Science, 283, 781-799.

Nimmo Smith, W. A. M., S. A. Thorpe, and A. Graham, 1999. Surface effects of bottom-generated turbulence in a shallow tidal sea. Nature, 400, 251-254.

Park, K., 1969. Oceanic CO_2 system: an evaluation of ten methods of investigation. Limnology and Oceanography, 14, 179-186.

Pritchard, D. W., 1967. What is an estuary: Physical viewpoint, 3-5. *In* G. H. Lauff (ed.), Estuaries. American Association for the Advancement of Science, Pub. No. 83, Washington DC.

Quay, P. D., B. Tillbrook, and C.S. Wong, 1992. Oceanic uptake of fossil fuel CO_2: carbon-13 evidence. Science, 256, 74-79.

Raymond, P. A. and J. J. Cole, 2001. Gas exchange in rivers and estuaries: Choosing a gas transfer velocity. Estuaries, 24(2), 312-317.

Richardson, T. L., G. A. Jackson, and A. B. Burd, 2003. Planktonic food web dynamics in two contrasting regions of Florida Bay, U. S. Bulletin of Marine Science, 73(3), 569-591.

Sugiura, Y., E. R. Ibert, and D. W. Wood, 1963. Mass transfer of carbon dioxide across sea surfaces. Journal of Marine Research, 21, 11-24.

Weiss, R. F., 1974. Carbon dioxide in water and seawater: The solubility of a non-ideal gas. Marine Chemistry, 2, 203-215.

Yates, K. K. and R. B. Halley, 2006. Diurnal variation in rates of calcification and carbonate sediment dissolution in Florida Bay. Estuaries and Coasts, 29(1), 24-39.

Zappa, C. J., W. R. McGillis, P. R. Raymond, J. E. Edson, E. J. Hintsa, H. J. Zemmelink, J. W. H. Dacey, and D. T. Ho, 2007. Environmental turbulent mixing controls on air-water gas exchange in marine and aquatic systems. Geophysical Research Letters, 34, L10601.

Appendix I

Floating Chamber Specifications

$F = (\partial pCO2/\partial t)(V/RTS)$

$(\partial pCO2/\partial t)$ = slope calculated from time series data

V = volume of system

hose volume = 4.7×10^{-4} m^3

headspace volume = 0.01222 m^3

cell volume = 1.19×10^{-5} m^3

total volume = 0.01270 m^3

R = universal gas constant = 8.2057459 x 10-5 m^3 atm k^{-1} mol^{-1}

T = temperature in Kelvin

S = surface area of bell = 0.1597 m^2

Appendix II

Carbon Dioxide System Chemistry

An understanding of CO_2 equilibria is essential to an understanding of carbon fluxes and distributions in the environment. The CO_2 system can be characterized by measuring at least two of the following four parameters (pCO_2, pH, TCO_2 and TA), while the remaining parameters can be calculated using thermodynamic relationships represented by the following equilibria:

$$CO_2(g) \overset{K_0}{\Leftrightarrow} CO_2(aq) \qquad \text{Eq. A1}$$

$$CO_2(aq) + H_2O \overset{K_H}{\Leftrightarrow} H_2CO_3 \qquad \text{Eq. A2}$$

$$CO_2 + H_2O \overset{K_1}{\Leftrightarrow} H^+ + HCO_3^- \qquad \text{Eq. A3}$$

$$HCO_3^- \overset{K_2}{\Leftrightarrow} H^+ + CO_3^{2-} \qquad \text{Eq. A4}$$

where the parameter K_0 is the solubility coefficient of carbon dioxide in seawater. The dissociation constants for Eq. 3 and Eq. 4 do not differentiate between $CO_2(aq)$ and H_2CO_3 and are more conveniently referred to as the sum of their concentrations denoted by $[CO_2^*]$. All quantities in brackets are concentrations in mol kg^{-1}.

The saturation states of aragonite (Ω_{Arg}) and calcite (Ω_{Cal}) are defined as

$$\Omega = [CO_3^{2-}][Ca^{2+}]/K_{sp} \quad \text{Eq. A5}$$

where K_{sp} is the solubility product for aragonite and calcite. K_{sp} values were taken from Mucci (1983), and calcium concentrations, assumed proportional to salinity, were calculated following Riley and Tongudai (1967).

The hydrogen ion concentration reported in this study is defined on the total H^+ concentration scale:

$$pH_T = -\log [H^+]_T \quad \text{Eq. A6}$$

where $[H^+]_T$ is the concentration of H^+ plus the concentration of HSO_4^- (DOE 1994). Seawater pH_T and pCO_2 was not directly measured in this study. As such, these values were calculated directly from TA and DIC.

The fugacity of CO_2 is defined by the relationship:

$$fCO2 = [CO_2^*]/K_0 \quad \text{Eq. A7}$$

where $[CO_2^*] = [CO_2(aq)] + [H_2CO_3]$. The first and second dissociation constant are defined by:

$$K_1 = [H^+]\,[HCO_3^-]/[CO_2] \quad \text{Eq. A8}$$

$$K_2 = [H^+]\,[CO_3^{2-}]/[HCO_3^-]. \quad \text{Eq. A9}$$

An equilibrium also exists between dissolved forms of CO_2 and inorganic carbon in solids

$$CaCO_3(s) \Leftrightarrow Ca^{2+} + CO_3^{2-}. \quad \text{Eq. A10}$$

Appendix III

CO_2 Flux Data Tables

Table A1. CO_2 flux data from 24 stations during the period April 9 to April 12, 2001.

Station	Date	Time (EST)	Latitude (DD)	Longitude (DD)	Air Temp. (˚C)	pCO_2 air (µatm)	CO_2 flux (mmol m^{-2} d^{-1})
East-01	n/d	n/d	n/d	n/d	n/d	n/d	n/d
East-02	4/9/01	11:40	25.2112	-80.4409	24.3	380	3.5
East-03	4/9/01	10:54	25.1537	-80.4240	23.9	377	-6.0
East-04	4/11/01	13:50	25.1953	-80.4937	25.7	379	11.2
East-05	4/11/01	14:31	25.1880	-80.5625	25.9	380	6.1
East-06	4/11/01	15:25	25.1470	-80.6047	25.9	382	33.1
East-07	4/11/09	12:53	25.1482	-80.5304	25.6	381	26.2
East-08	4/11/01	11:27	25.1281	-80.4767	25.3	376	34.0
East-09	4/11/01	15:50	25.1111	-80.6032	26.0	382	47.3
East-10	4/11/01	12:07	25.0958	-80.5269	25.4	378	34.4
East-11	4/12/01	17:30	25.1570	-80.6852	26.1	391	-9.2
North-01	4/12/01	14:08	25.1369	-80.7507	25.8	390	-21.3
North-02	4/12/01	12:58	25.1314	-80.8723	25.7	390	-24.3
North-03	4/12/01	12:17	25.1545	-80.8876	25.9	389	-14.7
Central-01	n/d	n/d	n/d	n/d	n/d	n/d	n/d
Central-02	4/12/01	13:40	25.0930	-80.7659	25.8	390	-35.1
Central-03	4/12/01	18:20	25.0383	-80.7181	26.1	391	-37.2
Central-04	4/12/01	10:30	24.9812	-80.7758	26.0	389	-33.0
Central-05	4/12/01	11:07	24.9877	-80.8560	26.0	389	-37.7
South-01	4/12/01	15:25	25.0421	-80.6050	25.9	391	10.6
South-02	4/12/01	16:30	25.0038	-80.6362	26.0	391	-9.4
South-03	4/12/01	9:59	24.9487	-80.6970	25.9	386	-7.1
South-04	4/13/01	11:04	24.8981	-80.7792	26.3	376	-18.1
South-05	4/13/01	11:47	24.9324	-80.8834	26.3	377	11.2

Table A2. CO_2 flux data from 24 stations during the period June 12 to June 15, 2001.

Station	Date	Time (EST)	Latitude (DD)	Longitude (DD)	Air Temp. (˚C)	pCO_2 air (µatm)	CO_2 flux (mmol m^{-2} d^{-1})
East-01	6/15/01	11:30	25.2330	-80.4637	29.1	377	-6.3
East-02	6/15/01	11:02	25.2139	-80.4399	29.1	376	-15.8
East-03	6/15/01	12:20	25.1598	-80.4205	29.1	378	5.2
East-04	6/12/01	13:05	25.1941	-80.4936	28.7	378	10.2
East-05	6/12/01	14:10	25.1876	-80.5633	28.7	379	2.3
East-06	6/12/01	16:00	25.1449	-80.6102	29.3	378	7.9
East-07	6/12/01	16:36	25.1460	-80.5430	29.6	380	4.0
East-08	6/12/01	17:10	25.1265	-80.4762	29.6	380	8.5
East-09	6/12/01	15:34	25.1047	-80.6002	29.3	379	6.3
East-10	6/15/01	14:45	25.0934	-80.5305	29.7	382	6.5
East-11	6/14/01	14:45	25.1576	-80.6830	29.8	383	2.3
North-01	6/13/01	11:25	25.1344	-80.7454	29.0	382	-9.6
North-02	6/13/01	13:00	25.1291	-80.8652	29.0	382	24.6
North-03	6/13/01	13:40	25.1633	-80.8814	29.4	383	18.6
Central-01	6/13/01	10:50	25.0750	-80.6750	29.0	382	-1.8
Central-02	6/13/01	12:07	25.0715	-80.7711	29.0	381	-15.5
Central-03	6/14/01	13:52	25.0382	-80.7175	30.2	382	-11.3
Central-04	6/13/01	17:10	24.9877	-80.7860	29.9	382	-15.2
Central-05	6/13/01	16:20	24.9988	-80.8843	29.6	382	-7.7
South-01	6/13/01	10:15	25.0385	-80.5988	28.8	379	2.0
South-02	6/14/01	13:24	25.0060	-80.6848	29.9	380	-17.5
South-03	6/13/01	18:00	24.9753	-80.6997	29.9	384	-5.4
South-04	6/14/01	11:35	24.9086	-80.7659	29.6	378	-9.2
South-05	6/14/01	12:14	24.9173	-80.8629	29.6	379	5.7

Table A3. CO_2 flux data from 24 stations during the period August 14 to August 17, 2001.

Station	Date	Time (EST)	Latitude (DD)	Longitude (DD)	Air Temp. (˚C)	pCO_2 air (µatm)	CO_2 flux (mmol m^{-2} d^{-1})
East-01	8/14/01	14:25	25.2349	-80.4620	29.9	367	55.6
East-02	8/14/01	13:47	25.2157	-80.4368	29.9	367	25.7
East-03	8/14/01	13:06	25.1595	-80.4203	29.7	366	2.9
East-04	8/14/01	15:55	25.1861	-80.4851	31.2	367	16.7
East-05	8/15/01	11:00	25.1880	-80.5623	29.4	368	1.6
East-06	8/15/01	11:45	25.1544	-80.6104	29.5	367	1.4
East-07	8/15/01	17:02	25.1101	-80.5427	30.4	365	2.8
East-08	8/15/01	17:27	25.1286	-80.4801	30.4	367	3.4
East-09	8/15/01	16:01	25.1155	-80.5896	30.7	366	1.0
East-10	n/d	n/d	n/d	n/d	n/d	n/d	n/d
East-11	8/15/01	13:00	25.1595	-80.4203	29.8	365	12.3
North-01	8/16/01	12:04	25.1333	-80.7505	29.9	364	3.7
North-02	8/16/01	13:32	25.1254	-80.8582	30.0	362	-19.2
North-03	8/16/01	14:00	25.1546	-80.8870	30.0	363	-19.9
Central-01	8/15/01	14:45	25.0788	-80.6690	32.4	366	-3.5
Central-02	8/16/01	12:35	25.0727	-80.7715	30.4	363	-5.6
Central-03	8/16/01	11:02	25.0371	-80.7191	29.7	364	-5.0
Central-04	8/16/01	16:51	24.9733	-80.8059	30.4	364	-14.8
Central-05	8/16/01	16:20	24.9955	-80.8832	30.5	362	-9.3
South-01	8/15/01	15:10	25.0302	-80.5894	32.4	365	-1.0
South-02	8/16/01	10:34	25.0057	-80.6837	29.7	364	-10.4
South-03	8/16/01	10:08	24.9529	-80.7003	29.5	365	18.2
South-04	8/17/01	10:21	24.9090	-80.7693	29.8	365	23.5
South-05	8/17/01	10:54	24.9176	-80.8572	30.0	364	3.8

Table A4. CO_2 flux data from 24 stations during the period November 13 to November 16, 2001.

Station	Date	Time (EST)	Latitude (DD)	Longitude (DD)	Air Temp. (°C)	pCO_2 air (µatm)	CO_2 flux (mmol m^{-2} d^{-1})
East-01	11/13/01	12:45	25.2344	-80.4604	23.3	391	15.1
East-02	11/13/01	13:20	25.2129	-80.4344	23.3	390	20.0
East-03	11/13/01	11:32	25.1566	-80.4144	22.5	391	30.8
East-04	11/14/01	10:12	25.1873	-80.4898	21.8	392	31.8
East-05	11/14/01	11:03	25.1910	-80.5627	21.8	391	15.7
East-06	11/14/01	11:42	25.1558	-80.5994	21.9	389	15.1
East-07	11/14/01	17:03	25.1209	-80.5267	22.2	389	29.1
East-08	11/15/01	9:10	25.1325	-80.4838	21.5	391	23.2
East-09	11/14/01	16:02	25.1143	-80.5865	21.9	385	22.3
East-10	11/15/01	9:44	25.0879	-80.5195	21.7	389	18.6
East-11	11/14/01	12:36	25.1597	-80.6752	21.9	388	0.8
North-01	11/16/01	15:55	25.1328	-80.7504	21.2	388	-3.8
North-02	11/16/01	14:40	25.1298	-80.8769	21.1	390	3.8
North-03	11/16/01	14:11	25.1503	-80.8896	20.8	387	-6.0
Central-01	11/14/01	13:36	25.0650	-80.6669	21.8	390	5.0
Central-02	11/16/01	15:26	25.0715	-80.7679	21.1	390	-40.3
Central-03	11/15/01	11:44	25.0390	-80.7174	21.7	387	-8.4
Central-04	11/16/01	10:12	24.9747	-80.7998	21.6	391	-13.5
Central-05	11/16/01	10:46	24.9890	-80.8695	21.5	391	-20.6
South-01	11/14/01	15:06	25.0238	-80.5880	21.6	390	12.9
South-02	11/15/01	12:13	25.0139	-80.6882	21.7	386	-8.4
South-03	11/15/01	12:34	24.9530	-80.7003	22.1	386	10.3
South-04	11/15/01	13:44	24.9051	-80.7523	22.1	386	7.3
South-05	n/d	n/d	n/d	n/d	n/d	n/d	n/d

Table A5. CO_2 flux data from 24 stations during the period December 11 to December 13, 2001.

Station	Date	Time (EST)	Latitude (DD)	Longitude (DD)	Air Temp. (°C)	pCO_2 air (µatm)	CO_2 flux (mmol m^{-2} d^{-1})
East-01	12/11/01	14:52	25.2328	-80.4581	24.5	394	51.0
East-02	12/11/01	14:07	25.2126	-80.4386	24.3	395	44.3
East-03	12/11/01	15:37	25.1562	-80.4239	25.8	395	46.6
East-04	12/11/01	11:16	25.2031	-80.4898	25.5	394	28.9
East-05	12/11/01	10:22	25.1892	-80.5642	24.9	395	18.2
East-06	12/11/01	9:24	25.1454	-80.6319	25.2	396	8.3
East-07	12/12/01	8:34	25.1465	-80.5252	24.8	395	24.7
East-08	12/11/01	14:24	25.1269	-80.4752	25.6	394	3.1
East-09	12/11/01	8:52	25.0995	-80.6032	25.2	397	21.2
East-10	12/12/01	9:34	25.0935	-80.5300	24.9	394	17.0
East-11	12/12/01	11:34	25.1585	-80.6840	25.1	393	1.8
North-01	12/12/01	12:18	25.1361	-80.7532	25.1	394	-19.4
North-02	12/12/01	13:49	25.1274	-80.8635	25.1	390	-4.7
North-03	12/12/01	14:24	25.1614	-80.8826	25.1	390	59.9
Central-01	12/12/01	10:50	25.0814	-80.6752	24.9	393	-4.2
Central-02	12/12/01	12:52	25.0696	-80.7717	25.1	390	-18.1
Central-03	12/13/01	9:41	25.0383	-80.7188	24.6	387	-8.6
Central-04	12/12/01	16:28	24.9835	-80.7881	25.2	387	14.9
Central-05	12/12/01	15:46	24.9934	-80.8734	25.2	387	-27.0
South-01	12/13/01	10:29	25.0446	-80.6076	24.6	387	5.4
South-02	12/13/01	11:11	25.0111	-80.6345	24.8	387	-5.2
South-03	12/13/01	9:03	24.9557	-80.7037	24.6	388	12.2
South-04	12/13/01	12:03	24.8953	-80.7664	24.9	387	33.4
South-05	n/d	n/d	n/d	n/d	n/d	n/d	n/d

Table A6. CO_2 flux data from 24 stations during the period April 2 to April 4, 2002.

Station	Date	Time (EST)	Latitude (DD)	Longitude (DD)	Air Temp. (˚C)	pCO_2 air (µatm)	CO_2 flux (mmol m^{-2} d^{-1})
East-01	4/2/02	14:40	25.2227	-80.4742	27.1	369	6.7
East-02	4/2/02	13:57	25.2076	-80.4376	26.5	368	10.0
East-03	4/2/02	11:26	25.1506	-80.4189	25.3	369	15.1
East-04	4/2/02	15:35	25.1980	-80.4857	26.5	369	15.0
East-05	4/2/02	16:16	25.1820	-80.5632	26.5	369	2.3
East-06	4/3/02	9:43	25.1655	-80.6150	26.2	368	3.0
East-07	4/3/02	9:09	25.1357	-80.5457	25.4	368	7.0
East-08	4/2/02	16:58	25.1264	-80.4718	25.3	369	7.4
East-09	4/4/02	8:34	25.1017	-80.6030	25.5	375	10.3
East-10	4/3/02	8:26	25.0667	-80.5113	25.4	367	1.6
East-11	4/3/02	10:19	25.1579	-80.6787	25.8	368	2.5
North-01	4/3/02	11:16	25.1374	-80.7569	25.8	368	0.0
North-02	4/3/02	12:11	25.1236	-80.8538	26.4	371	1.2
North-03	4/3/02	12:57	25.1662	-80.8796	26.6	367	5.7
Central-01	4/4/02	9:19	25.0849	-80.6639	25.6	377	-0.1
Central-02	4/4/02	9:56	25.0732	-80.7607	26.0	380	-5.2
Central-03	4/4/02	10:42	25.0348	-80.7198	24.0	381	-1.1
Central-04	4/4/02	11:27	24.9786	-80.7898	24.4	374	-4.1
Central-05	4/3/02	15:15	24.9918	-80.8705	24.4	369	-9.2
South-01	4/4/02	14:04	25.0351	-80.5988	24.0	374	-0.7
South-02	4/4/02	13:24	25.0168	-80.6363	24.2	372	-1.6
South-03	4/4/02	12:02	24.9460	-80.7188	24.5	371	0.9
South-04	4/3/02	17:01	24.8829	-80.8094	24.6	368	-1.0
South-05	4/3/02	16:23	24.9151	-80.9011	25.1	371	4.0

Table A7. CO_2 flux data from 24 stations during the period October 22 to October 24, 2002.

Station	Date	Time (EST)	Latitude (DD)	Longitude (DD)	Air Temp. (˚C)	pCO_2 air (µatm)	CO_2 flux (mmol m^{-2} d^{-1})
East-01	10/22/02	11:40	25.2279	-80.4607	25.5	365	14.4
East-02	10/22/02	10:39	25.2126	-80.4386	25.7	367	8.2
East-03	10/22/02	12:09	25.1589	-80.4228	25.5	363	22.0
East-04	10/22/02	13:01	25.2056	-80.4878	25.7	362	14.2
East-05	10/22/02	13:32	25.1930	-80.5619	25.9	361	5.3
East-06	10/22/02	14:04	25.1469	-80.6379	25.9	364	3.1
East-07	10/22/02	16:19	25.1488	-80.5273	26.3	360	2.2
East-08	10/22/02	17:39	25.1239	-80.4746	26.8	362	11.3
East-09	10/22/02	15:39	25.0953	-80.6015	26.3	362	0.0
East-10	10/22/02	16:42	25.0942	-80.5296	26.5	361	2.9
East-11	10/23/02	9:53	25.1574	-80.6835	26.4	374	11.0
North-01	10/23/02	12:04	25.1355	-80.7538	26.5	365	-0.4
North-02	10/23/02	12:38	25.1263	-80.8610	26.5	366	-4.1
North-03	10/23/02	13:32	25.1476	-80.8918	27.1	365	-9.9
Central-01	10/23/02	9:18	25.0793	-80.6753	26.3	379	-1.3
Central-02	10/23/02	11:35	25.0696	-80.7713	26.5	369	-4.2
Central-03	10/23/02	10:40	25.0366	-80.7183	26.7	373	-0.1
Central-04	10/23/02	16:36	24.9843	-80.7846	27.7	362	10.7
Central-05	10/23/02	16:06	24.9936	-80.8713	27.7	363	-2.8
South-01	10/22/02	15:13	25.0432	-80.6060	26.0	360	6.1
South-02	10/22/02	14:45	25.0112	-80.6324	26.0	361	0.6
South-03	10/23/02	17:05	24.9561	-80.7023	27.7	364	2.2
South-04	10/24/02	9:51	24.8912	-80.7779	27.2	366	29.3
South-05	10/24/02	10:35	24.9137	-80.8583	26.4	366	1.1

Table A8. CO_2 flux data from 24 stations during the period February 11 to February 13, 2003.

Station	Date	Time (EST)	Latitude (DD)	Longitude (DD)	Air Temp. (˚C)	pCO_2 air (µatm)	CO_2 flux (mmol m^{-2} d^{-1})
East-01	2/13/03	10:24	25.2291	-80.4602	18.7	377	5.7
East-02	2/13/03	11:17	25.2102	-80.4417	18.4	377	10.1
East-03	2/13/03	11:42	25.1780	-80.4195	18.3	378	23.7
East-04	2/11/03	11:10	25.1801	-80.4799	21.3	380	14.7
East-05	2/11/03	11:38	25.1933	-80.5481	20.5	380	2.9
East-06	2/11/03	12:12	25.1647	-80.6150	20.5	377	10.1
East-07	2/11/03	10:41	25.1481	-80.5258	21.3	381	17.4
East-08	2/11/03	16:10	25.1247	-80.4752	20.2	375	25.1
East-09	2/11/03	15:36	25.0966	-80.5869	20.2	374	15.5
East-10	2/11/03	10:05	25.0890	-80.5280	21.9	383	19.8
East-11	2/11/03	12:49	25.1477	-80.6847	19.8	375	12.8
North-01	2/12/03	12:42	25.1250	-80.7528	17.9	375	-0.3
North-02	2/12/03	13:21	25.1236	-80.8537	17.9	375	5.6
North-03	2/12/03	13:55	25.1564	-80.8862	18.4	374	34.4
Central-01	2/11/03	13:29	25.0669	-80.6734	19.8	377	5.0
Central-02	2/12/03	12:10	25.0794	-80.7600	18.0	375	2.1
Central-03	2/12/03	11:23	25.0371	-80.7194	19.1	380	2.0
Central-04	2/12/03	10:39	24.9856	-80.7805	19.1	382	-2.8
Central-05	2/12/03	16:16	24.9849	-80.8708	19.7	376	-10.6
South-01	2/11/03	14:39	25.0300	-80.6026	19.4	375	12.4
South-02	2/11/03	14:06	25.0158	-80.6376	19.4	373	9.8
South-03	2/12/03	10:01	24.9386	-80.7128	20.1	384	18.1
South-04	2/12/03	17:25	24.8856	-80.7931	20.2	377	1.9
South-05	2/12/03	16:57	24.8989	-80.8733	20.2	377	-3.5

Table A9. CO_2 flux data from 24 stations during the period April 22 to April 23, 2003.

Station	Date	Time (EST)	Latitude (DD)	Longitude (DD)	Air Temp. (˚C)	pCO_2 air (µatm)	CO_2 flux (mmol m^{-2} d^{-1})
East-01	4/22/03	10:29	25.2248	-80.4673	23.8	376	2.9
East-02	4/22/03	10:55	25.2131	-80.4375	23.9	375	6.7
East-03	4/22/03	9:34	25.1566	-80.4240	23.8	376	1.8
East-04	4/22/03	13:00	25.2025	-80.4887	26.5	375	10.6
East-05	4/22/03	15:03	25.1873	-80.5636	24.6	372	-2.8
East-06	4/22/03	16:55	25.1455	-80.6319	25.1	370	4.9
East-07	4/22/03	14:19	25.1456	-80.5252	24.6	375	26.5
East-08	4/22/03	18:04	25.1277	-80.4751	25.2	371	14.9
East-09	4/22/03	16:08	25.0969	-80.6019	24.8	372	28.0
East-10	4/22/03	13:49	25.0927	-80.5293	24.6	375	34.8
East-11	4/23/03	10:06	25.1575	-80.6817	24.5	376	-15.1
North-01	4/23/03	13:01	25.1257	-80.7684	23.8	373	-0.6
North-02	4/23/03	13:41	25.1307	-80.8755	23.7	373	7.3
North-03	4/23/03	14:48	25.1607	-80.8831	24.0	371	11.2
Central-01	4/23/03	9:24	25.0795	-80.6762	24.4	377	-26.0
Central-02	4/23/03	12:34	25.0689	-80.7728	23.8	374	-27.6
Central-03	4/23/03	12:05	25.0369	-80.7204	24.2	376	-19.2
Central-04	4/23/03	17:03	24.9847	-80.7876	24.7	376	-34.8
Central-05	4/23/03	16:33	24.9936	-80.8729	24.7	373	-31.0
South-01	4/23/03	8:48	25.0448	-80.6078	24.4	378	-17.0
South-02	4/23/03	11:26	25.0125	-80.6326	24.5	375	-13.7
South-03	n/d	n/d	n/d	n/d	n/d	n/d	n/d
South-04	4/23/03	19:06	24.8955	-80.7658	25.2	372	-28.9
South-05	4/23/03	18:22	24.9158	-80.8579	25.0	374	-11.4

Appendix IV

Carbonate System Data Tables

Table A10. Carbonate system parameters from 24 stations during the period April 2 to April 4, 2002.

Station	Salinity	water temp (˚C)	DIC (µmol kg^{-1})	TA (µmol kg^{-1})	pCO_2 (µatm)	pH_T	Ω_{Arg}	Ω_{Cal}
East-01	20.9	28.3	2670.4	2984.5	502.7	8.123	4.5	7.2
East-02	25.1	27.9	2484.5	2792.3	494.9	8.080	4.2	6.5
East-03	29.4	27.6	2565.1	2879.4	566.8	8.021	4.2	6.3
East-04	27.0	28.5	2473.6	2833.7	440.8	8.116	4.8	7.4
East-05	24.5	28.4	2462.0	2836.9	387.2	8.176	5.1	7.9
East-06	22.3	26.9	2468.0	2796.7	403.3	8.170	4.5	7.2
East-07	25.7	26.6	2404.0	2699.0	471.1	8.082	3.9	6.1
East-08	26.5	27.9	2410.8	2731.8	462.9	8.088	4.3	6.6
East-09	23.9	26.5	2535.0	2791.3	573.9	8.032	3.6	5.6
East-10	26.9	26.5	2217.6	2556.5	354.5	8.157	4.3	6.7
East-11	25.7	27.1	2463.1	2821.3	401.6	8.155	4.8	7.4
North-01	29.2	27.7	2331.3	2725.6	361.7	8.161	5.0	7.7
North-02	34.3	28.3	2303.8	2715.7	392.6	8.109	5.0	7.5
North-03	33.8	30.2	2485.1	2893.4	487.8	8.056	5.1	7.7
Central-01	26.4	27.2	2240.1	2608.8	330.5	8.191	4.8	7.4
Central-02	32.8	27.2	1989.6	2554.6	172.7	8.365	6.6	10.0
Central-03	30.6	27.6	2199.1	2693.2	247.1	8.278	6.1	9.3
Central-04	34.5	28.4	1764.6	2320.4	152.2	8.361	6.2	9.3
Central-05	33.0	28.2	1915.4	2485.5	164.7	8.367	6.6	10.0
South-01	28.3	29.1	2212.3	2542.0	420.6	8.086	4.2	6.5
South-02	29.8	29.5	2075.4	2473.3	311.8	8.172	4.9	7.5
South-03	33.6	28.7	2109.7	2478.8	380.5	8.089	4.4	6.6
South-04	33.4	27.6	2083.7	2551.7	258.7	8.231	5.5	8.3
South-05	33.1	27.3	2345.8	2689.3	472.2	8.047	4.2	6.4

Table A11. Carbonate system parameters from 24 stations during the period October 22 to October 24, 2002.

Station	Salinity	water temp (˚C)	DIC (µmol kg^{-1})	TA (µmol kg^{-1})	pCO_2 (µatm)	pH_T	Ω_{Arg}	Ω_{Cal}
East-01	14.8	27.9	2968.3	3170.3	798.5	8.014	3.4	5.5
East-02	18.6	26.8	2724.4	2981.6	572.7	8.090	3.8	6.2
East-03	27.4	27.6	2599.0	2836.0	741.7	7.926	3.3	5.1
East-04	25.6	29.0	2493.5	n/d	n/d	n/d	n/d	n/d
East-05	17.5	29.2	2282.9	2579.3	374.9	8.198	4.3	7.0
East-06	14.8	28.9	2310.6	2566.7	413.0	8.182	3.9	6.4
East-07	21.5	29.3	2222.9	2534.7	378.5	8.161	4.3	6.8
East-08	28.3	28.7	2166.4	2435.6	502.9	8.007	3.5	5.3
East-09	23.6	28.5	1956.2	2300.1	269.9	8.231	4.5	7.0
East-10	27.2	28.3	1950.7	2243.2	360.8	8.101	3.7	5.6
East-11	18.1	27.7	2487.3	2717.1	557.1	8.069	3.4	5.5
North-01	23.1	28.5	2151.5	2458.5	367.3	8.151	4.1	6.5
North-02	34.0	28.7	2031.3	2508.3	254.5	8.226	5.6	8.4
North-03	33.0	30.0	2094.9	2552.0	294.0	8.187	5.5	8.2
Central-01	26.7	27.3	2106.0	2434.3	343.2	8.151	4.2	6.5
Central-02	24.9	27.7	2163.9	2564.0	272.0	8.260	5.2	8.1
Central-03	29.3	27.7	2158.0	2511.6	358.3	8.134	4.4	6.7
Central-04	35.1	28.9	2156.4	2489.2	471.0	8.011	3.9	5.9
Central-05	33.7	28.7	2089.3	2492.3	334.9	8.134	4.8	7.2
South-01	27.3	28.8	2026.6	2328.4	381.6	8.094	3.8	5.9
South-02	30.9	28.7	2005.3	2351.0	348.9	8.111	4.2	6.3
South-03	34.9	28.5	2026.3	2375.5	388.3	8.062	4.0	6.1
South-04	37.1	27.7	2119.2	2408.4	539.0	7.946	3.3	5.0
South-05	37.3	27.5	1935.7	2287.1	363.0	8.065	3.8	5.8

Table A12. Carbonate system parameters from 24 stations during the period February 11 to February 13, 2003.

Station	Salinity	water temp (˚C)	DIC (µmol kg^{-1})	TA (µmol kg^{-1})	pCO_2 (µatm)	pH_T	Ω_{Arg}	Ω_{Cal}
East-01	24.8	21.1	2653.1	2966.0	412.7	8.171	4.1	6.6
East-02	26.7	21.3	2659.8	2985.7	420.1	8.157	4.3	6.7
East-03	30.2	22.2	2724.6	3096.9	428.9	8.147	4.7	7.3
East-04	28.3	24.3	2795.4	3071.0	649.8	8.001	3.7	5.8
East-05	24.0	24.5	2584.2	2915.3	414.7	8.167	4.5	7.1
East-06	23.2	24.8	2673.0	2954.6	524.3	8.091	3.9	6.2
East-07	27.1	24.1	2789.6	3032.1	708.9	7.969	3.4	5.2
East-08	28.1	25.6	2703.9	2963.0	683.8	7.969	3.5	5.5
East-09	26.2	25.3	2596.6	2877.0	551.5	8.046	3.8	5.9
East-10	28.1	24.2	2620.7	2886.1	596.9	8.009	3.5	5.5
East-11	28.4	25.0	2926.8	3239.6	637.3	8.028	4.3	6.6
North-01	33.7	22.6	2608.2	3032.0	375.8	8.172	5.1	7.9
North-02	31.9	23.5	2785.8	3170.9	473.6	8.113	4.9	7.5
North-03	31.5	21.9	2861.1	3104.4	752.3	7.937	3.2	5.0
Central-01	32.2	25.4	2757.4	3109.4	560.7	8.043	4.5	6.9
Central-02	32.7	23.2	2625.1	3020.5	413.6	8.140	4.9	7.5
Central-03	33.6	22.9	2668.3	3099.5	388.1	8.169	5.3	8.1
Central-04	36.4	23.5	2438.9	2851.9	380.0	8.136	4.8	7.3
Central-05	31.7	24.3	2273.8	2722.4	271.8	8.250	5.4	8.3
South-01	30.9	25.8	2682.2	2984.2	620.8	7.996	4.0	6.0
South-02	32.0	25.7	2709.9	3015.9	638.3	7.986	4.0	6.0
South-03	33.4	23.2	n/d	2868.2	n/d	n/d	n/d	n/d
South-04	31.4	24.4	2336.0	2716.7	352.2	8.162	4.6	7.1
South-05	32.0	23.9	2258.1	2678.8	289.4	8.223	5.0	7.7

Table A13. Carbonate system parameters from 24 stations during the period April 22 to April 23, 2003.

Station	Salinity	water temp (˚C)	DIC (µmol kg^{-1})	TA (µmol kg^{-1})	pCO_2 (µatm)	pH_T	Ω_{Arg}	Ω_{Cal}
East-01	28.5	26.6	2294.9	2606.3	438.2	8.081	4.0	6.1
East-02	30.5	27.1	2308.1	2633.1	453.3	8.064	4.1	6.2
East-03	31.9	26.5	2417.7	2807.3	403.1	8.123	4.8	7.4
East-04	31.3	27.6	2482.5	2831.9	496.6	8.055	4.5	6.8
East-05	28.6	28.2	2309.9	2688.6	375.1	8.146	4.9	7.4
East-06	28.1	28.3	2252.5	2582.5	418.7	8.095	4.3	6.5
East-07	31.4	27.9	2486.8	2769.2	640.9	7.954	3.7	5.6
East-08	31.6	28.0	2337.0	2654.6	507.9	8.021	4.0	6.0
East-09	30.9	28.0	2394.0	2676.2	594.3	7.970	3.6	5.5
East-10	31.7	27.6	2482.2	2749.7	673.6	7.932	3.5	5.3
East-11	33.8	26.5	1921.9	2369.3	227.1	8.249	5.1	7.7
North-01	36.1	28.3	2058.4	2496.2	306.4	8.156	5.0	7.5
North-02	34.0	28.2	2525.3	2915.7	493.3	8.057	4.9	7.3
North-03	34.6	29.3	2492.3	2925.5	449.0	8.087	5.3	8.0
Central-01	34.0	26.8	1799.8	2301.8	171.4	8.328	5.6	8.5
Central-02	35.8	28.3	1466.9	2187.3	65.6	8.582	7.6	11.3
Central-03	35.2	27.4	1519.8	2092.8	103.4	8.444	6.0	9.1
Central-04	36.5	28.3	1602.8	2225.9	108.2	8.442	6.6	9.9
Central-05	34.1	27.9	1823.5	2371.6	161.3	8.354	6.2	9.3
South-01	34.1	26.6	1939.0	2353.5	259.9	8.201	4.7	7.1
South-02	34.9	26.9	1804.6	2293.0	185.2	8.298	5.4	8.1
South-03	34.8	27.7	1744.8	2178.2	212.3	8.235	4.7	7.1
South-04	35.8	27.9	1808.7	2296.7	199.0	8.270	5.4	8.0
South-05	34.4	27.7	2060.0	2522.7	265.2	8.215	5.4	8.1

Appendix V

Error in Calculated CO_2 System Parameters

Uncertainty in both the measured CO_2 parameters, TA and DIC, as well as uncertainties in the various equilibrium constants required to calculate all additional CO_2 parameters have been shown to produce significant errors in CO_2 system calculations. Millero (2007) reported probable errors in calculated parameters in terms of uncertainties in calculated values as pH (+/-0.0062) and pCO_2 (+/-5.7 µatm) using total alkalinity (+/- 3 µmol kg^{-1}) and dissolved inorganic carbon (+/- 2 µmol kg^{-1}) as input parameters. In this study, uncertainties in total alkalinity (+/- 3.7 µmol kg^{-1}) and dissolved inorganic carbon (+/- 6.7 µmol kg^{-1}) have the potential to produce even larger errors in calculated carbonate system parameters. Due to the highly variable nature of estuarine waters, and the lack of a third parameter to examine internal consistencies in calculated values, it is safe to assume that the above estimated probable errors in calculated values represent a best case scenario for the data presented here.